Universidade de Aveiro
2015

Secção Autónoma de Ciências da Saúde

Helder Luís da Costa Alves

O impacto do Aβ no complexo Neurabina/PP1

The impact of Aβ on the Neurabin/PP1 complex

Universidade de Aveiro
2015

Secção Autónoma de Ciências da Saúde

Helder Luís da Costa Alves

O impacto do Aβ no complexo Neurabina/PP1

The impact of Aβ on the Neurabin/PP1 complex

Dissertação apresentada à Universidade de Aveiro para cumprimento dos requisitos necessários à obtenção do grau de Mestre em Biomedicina Molecular, realizada sob a orientação científica da Professora Doutora Odete Abreu Beirão da Cruz e Silva, Professora Auxiliar com Agregação da Secção Autónoma de Ciências da Saúde da Universidade de Aveiro.

Este trabalho contou com o apoio do grupo de Neurociências e Sinalização Celular do iBiMED, SACS, e pelo Centro de Biologia Celular (CBC) da Universidade de Aveiro, e foi financiado pelos fundos JPND/0006/2011 BiomarKAPDua e PEST-OE/SAU/UI0482/2011.

Dedico esta dissertação aos meus pais pelo amor, educação, motivação, dedicação e apoio que me deram ao longo de toda a vida.

o júri

presidente

Professora Doutora Ana Gabriela da Silva Cavaleiro Henriques
Professora Auxiliar Convidada, Universidade de Aveiro

Professora Doutora Etelvina Maria de Almeida Paula Figueira
Professora Auxiliar, Universidade de Aveiro

Professora Doutora Odete Abreu Beirão da Cruz e Silva
Professora Auxiliar com Agregação, Universidade de Aveiro

agradecimentos

Gostaria de agradecer à Professora Doutora Odete da Cruz e Silva pela oportunidade de realizar este trabalho no laboratório de neurociências e por toda a sua orientação, encorajamento e conselhos durante a realização desta dissertação.

À Professora Doutora Ana Gabriela Henriques por todo o apoio e ajuda que sempre disponibilizou durante a realização desta dissertação.

A todos os meus colegas do laboratório de neurociências que sempre tornaram o ambiente do laboratório amigável e convidativo, e que nunca rejeitaram um pedido de ajuda.

À "minha" bancada. À Oli, um imensurável obrigado, por todo o auxílio, apoio, ensinamentos, amizade e disponibilidade que todos os dias demonstrou, tornando esta experiência muito mais agradável. À Lili pela diversão, apoio, companhia e amizade que também demonstrou. À Catarina pela companhia na "viagem" e por toda a ajuda.

Às outras bancadas. À Pipa, à Rochinha e ao Roberto pela ajuda, simpatia e companhia ao longo do ano. À Marote pelos húngaros e broas de mel.

Aos meus companheiros e amigos de licenciatura e mestrado. Ao Zé, Sérgio, Márcio por estes 5 anos vividos com muito companheirismo e amizade. À Serrano e à Soraia por toda a ajuda, pelos bons momentos vividos e pela companhia.

À Ana, pelo apoio incondicional durante estes 4 anos.

E, principalmente, aos meus pais, aos meus irmãos e à minha família, por tudo.

palavras-chave

Aβ, doença de Alzheimer, neurabina-1, neurabina-2, PP1, interacção, células SH-SY5Y, diferenciação, co-localização

resumo

O nosso cérebro é uma estrutura complexa constituída por neurónios capazes de comunicar entre si através de sinapses, que geralmente ocorrem entre o terminal axonal e a espinha dendrítica de dois neurónios. Estas espinhas dendríticas são dinâmicas, permitindo assim que se adaptem aos estímulos que recebem, quer estimulantes quer inibitórios. A PP1 é uma proteína fosfatase que catalisa grande parte das reações de desfosforilação que ocorrem no nosso corpo, encontrando-se envolvida, por isso, em diversas funções, desde o metabolismo do glicogénio até à regulação sináptica. As neurabinas são duas proteínas estrutural e funcionalmente similares, muito concentradas nas espinhas dendríticas, onde interagem com diversas proteínas, incluindo a PP1, e as direcionam ou para os recetores que aqui se encontram, ou para o citoesqueleto de actina ou para outras regiões do neurónio. Assim, as neurabinas são responsáveis pela regulação da morfologia neuronal, pela transmissão sináptica e, por conseguinte, pela plasticidade sináptica. A doença de Alzheimer é a doença neurodegenerativa mais comum e é caraterizada por depósitos de Aβ e presença de tranças neurofibrilares, pela destruição de sinapses e morte neuronal, e pela perda gradual da memória e de outras funções cognitivas. A PPA é uma proteína transmembranar que, na doença de Alzheimer, é processada anormalmente pela via amiloidogénica, resultando na sobreprodução de Aβ, um peptídeo tóxico, que se crê ser o principal causador das alterações caraterísticas da doença de Alzheimer.

O principal objetivo desta tese de mestrado foi avaliar o efeito do Aβ na expressão das neurabinas e na interação destas com a PP1. Os resultados aqui reportados demonstram uma ligeira diminuição de ambas as neurabinas quando o Aβ se encontra presente nas células, provavelmente pelas alterações a nível morfológico e destruição de sinapses que ocorre. Também foi aqui reportado que o Aβ interfere com o complexo neurabina-1/PP1, talvez pelo efeito direto do Aβ na neurabina-1 ou pela desregulação de fosfatases e cinases existente quando o Aβ se encontra presente no meio, levando a uma diminuição da afinidade entre a neurabina-1 e a PP1. O mesmo efeito não se verificou no complexo neurabina-2/PP1, talvez por serem reguladas de forma diferente por diferentes cinases. O estudo imunocitoquímico não demonstrou alterações a nível da co-localização entre a neurabina-1 e a PP1, e permitiu a caraterização da distribuição celular de ambas as neurabinas em células SH-SY5Y.

As experiências laboratoriais realizadas nesta tese permitiram concluir que o Aβ interfere com a expressão das neurabinas e com o complexo neurabina-1/PP1. No entanto, terão que ser realizados estudos adicionais para compreender a relevância fisiológica do complexo neurabina-1/PP1.

keywords

Aβ, Alzheimer's disease, neurabin-1, neurabin-2, PP1, interaction, SH-SY5Y cells, differentiation, co-localization

abstract

Our brain is a complex structure constituted by neurons capable of communicating through synapses, which generally occur between the axon terminal and the dendritic spine of two different neurons. These dendritic spines are dynamic, which allow for the rapid adaptation to the different stimuli they receive. PP1 is a phosphatase protein which catalyzes the majority of dephosphorylation reactions that occur in our body. It is involved in several different functions, from glycogen metabolism to synaptic regulation. Neurabins are two structurally and functionally similar proteins, highly concentrated in dendritic spines, where they interact with several proteins – PP1 included –, and target them to receptors, the cytoskeleton and to other cellular compartments. Thus, neurabins regulate neuronal morphology and synaptic transmission, and hence, synaptic plasticity. Alzheimer's disease is the most common neurodegenerative disease and it is characterized by the deposition of Aβ and the presence of neurofibrilliary tangles, by the loss of synapses and neuronal death, and by the gradual loss of memory and other cognitive functions. APP is an integral membrane protein which, in Alzheimer's disease, is abnormally cleaved via the amyloidogenic pathway, thus resulting in the overproduction of a toxic peptide, Aβ, believed to be the major culprit of the changes observed in this disease.

The main aim of this thesis was to study the effects of Aβ on neurabins expression and to evaluate its effects on the neurabin/PP1 complex. The results here reported showed a slight decrease in both neurabins expression levels when Aβ was added to the cells, possibly due to the morphological changes and synaptic dysfunction this peptide induces. It was also here reported that Aβ interferes with the neurabin-1/PP1 complex. This may be related to the direct effect of Aβ on neurabin-1 or due to the imbalance of phosphatases and kinases seen when Aβ is added, which could result in a decrease of neurabin-1's affinity for PP1. The same effect was not seen with the neurabin-2/PP1 complex, possibly because they are differently regulated by several kinases. The immunocytochemistry study here performed did not show any changes between the co-localization of neurabin-1 and PP1, and allowed for assessment of cellular distribution of neurabin-1 and neurabin-2 in SH-SY5Y cells.

The experimental procedures here performed allowed us to conclude that Aβ interferes with the expression of both neurabins and with the interaction between neurabin-1 and PP1. However, additional studies need to be conducted in order to understand the physiological relevance of this complex.

Index

List of figures

List of tables

Abbreviations

3^{rd} iL	3^{rd} intracellular loop
a.a.	Amino acids
Aβ	Amyloid β-peptide
$\alpha_{1/2\text{-A/B}}$ AR	$\alpha_{1/2\text{-A/B}}$ adrenergic receptor
AD	Alzheimer's disease
AICD	Amyloid precursor protein intracellular domain
AMPA	α-amino-3-hydroxy-5-methyl-4-isoxazole propionic acid
APLP1	APP-like protein 1
APLP2	APP-like protein 2
ApoE	Apolipoprotein E
APP	Amyloid β precursor protein
APS	Ammonium persulfate
ATP	Adenosine 5'-triphosphate
BCA	Bicinchoninic acid
BSA	Bovine serum albumin
C83	C-terminal fragment consisting of 83 a.a.
C99	C-terminal fragment consisting of 99 a.a.
Ca^{2+}	Calcium
CaMKII	Calmodulin-dependent protein kinase II
CCKA/B	Cholecystokinin receptor type A/B
Cdk5	Cyclin-dependent-like kinase 5
Co-IP	Co-immunoprecipitation
Cyt c	Cytochrome C
D2	D(2) dopamine receptor
DCAMKL1	Serine/threonine-protein kinase DCLK1
Dcx	Doublecortin
ECL	Enhanced chemiluminesce
ERK2	Extracellular signal-regulated kinase 2
DARPP32	Dopamine- and cAMP-regulated neuronal phosphoprotein
FBS	Fetal bovine serum
HBSS	Hank's Balanced Salt Solution
I-2	Protein phosphatase inhibitor 2
ICC	Immunocytochemistry

KPI	Kunitz protease inhibitor
LB	Loading buffer
Lfc	Rho guanine nucleotide exchange factor 2
LGB	Lower gel buffer
LTD	Long-term depression
LTP	Long-term potentiation
M1/2/3	Muscarinic acetylcholine receptor M1/2/3
MAP2	Microtubule-associated protein 2
MEM	Minimal Essential Medium
Mypt1	Myosin phosphatase-targeting subunit 1
NFT	Neurofibrilliary tangles
NMDA	N-methyl-D-aspartate
PBS	Phosphate buffered saline
PDZ	PSD-95/Dlg/ZO-1
PIP	PP1-interacting proteins
PKA	cAMP-dependent protein kinase catalytic subunit alpha
PP1	Protein phosphatase 1
PSD	Postsynaptic density
R4-RGS	R4 subfamily of RGS proteins
RA	Retinoic acid
Rac3	Ras-related C3 botulinum toxin substrate
Ras-GRF1	Ras-specific guanine nucleotide-releasing factor 1
RGS	Regulators of G protein signaling
SAM	Sterile alpha domain
SDS	Sodium dodecylsulfate
SDS-PAGE	SDS-polyacrylamide gel electrophoresis
Ser/Thr	Serine/Threonine
TBS	Tris-Buffered Saline
TBS-T	Tris-Buffered Saline Tween
TGN38	Trans-Golgi network integral membrane protein TGN38
Tiam1	T-lymphoma invasion and metastasis-inducing protein 1
UGB	Upper gel buffer
WB	Western blot

1. Introduction

The human brain. A highly complex structure that governs our lives. Within it lies everything we do, think and feel. It dictates how we react in front of our family, our loved ones, and even in front of a perilous situation. It is the command center of all our actions, thoughts, memories and emotions. Such complex structure needs a highly organized interconnected network to guarantee that its functions are properly executed.

This network is constituted by neurons (and also supporting glial cells) capable of communicating with each other through synapses, especially chemical synapses. Chemical synapses rely on the transfer of endogenous chemical compounds – neurotransmitters – between a pre- and a postsynaptic neuron. These neurotransmitters are produced on the presynaptic neuron and wrapped in membrane-bounded organelles – synaptic vesicles -, which are then secreted to the synaptic cleft. After diffusing across the synaptic cleft, neurotransmitters bind to specific receptors present on the membrane of the postsynaptic neuron [1] (Figure 1).

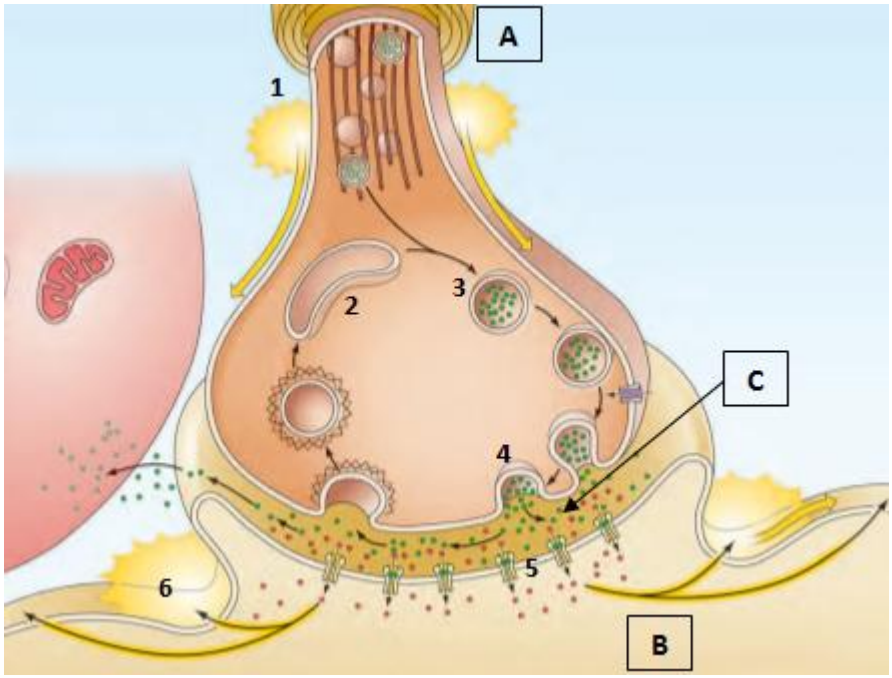

Figure 1 – Chemical synapse. An action potential invades the presynaptic terminal (A) and there is the production of neurotransmitters (1). A synaptic vesicle is formed (2), wraps the newly-formed neurotransmitters (3), which are then released into the synaptic cleft (4). Here they bind to receptors (5) and then cause an excitatory or inhibitory potential that changes the excitability of the postsynaptic neuron (6). A, presynaptic neuron; B, postsynaptic neuron; C, synaptic cleft (adapted from [1]).

1.1. Dendritic spines

The type of neuronal communication, mentioned above, usually occurs between an axon terminal (presynaptic component) and dendritic spines (postsynaptic component). Dendritic spines are membranous protrusions composed of a spine head and a spine neck which arise from the dendritic shaft [2,3]. These dendritic spines are present on different populations of neurons in the brain and are preferentially located on the peripheral dendrites of neocortical and hippocampal pyramidal neurons, on the striatum and in cerebellar Purkinje cells [2,4]. They are thought to be key structures in both learning and memory formation, as they receive the majority of excitatory and inhibitory outputs in the central nervous system [2,5].

1.1.1. Structure and Composition

Dendritic spines can be classified in three major types: thin ("thin spines"), short without a well-defined spine deck ("stubby spines") or with a large bulbous head ("mushroom spines") [2–4,6] (Figure 2). However, dendritic spines are not static, i.e., they do not always have the same structure, since in developing neurons, the majority of dendritic spines change their shape over periods of minutes or hours. As for dendritic spines in mature neurons, they are not as motile as in developing neurons and thus, there are fewer changes in their shape. Larger spines (mushroom spines, for example) are functionally stronger in their response to glutamate, regulation of intracellular calcium, protein translation and degradation, and endosomal recycling than smaller spines, which are more flexible, rapidly enlarging or shrinking in response to subsequent activation [6,7].

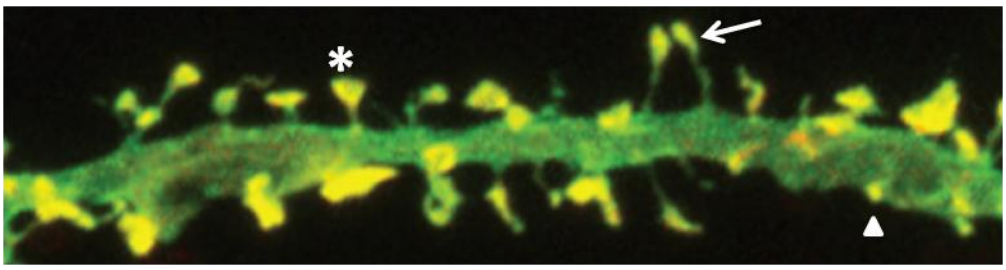

Figure 2 – Dendritic spine morphology. It is possible to distinguish several types of dendritic spines (yellow). Arrow, arrowhead and asterisk, represent thin, stubby and mushroom spines, respectively (adapted from [6]).

The first structure of the dendritic spine, and probably the most complex spine organelle, is the postsynaptic density (PSD), an electron-dense thickening of the postsynaptic membrane that harbors hundreds of proteins involved in synaptic plasticity, including neurotransmitter receptors, such as N-methyl-ᴅ-aspartate (NMDA) receptors, α-amino-3-hydroxy-5-methyl-4-isoxazole

propionic acid (AMPA) receptors, kainaite and metabotropic glutamate receptors, along with numerous signaling and scaffolding proteins [2,4,7,8].

Below the PSD we can find both monomeric (globular, G-actin) and filamentous (F-actin) actin. The spines' cytoskeleton is rich in F-actin, which modulates spine head structure in response to postsynaptic signaling and contributes to the overall structure of synapses. It organizes the PSD, anchoring and stabilizing postsynaptic receptors and localizing the translation machinery. The dendritic spine is rich in actin-binding proteins, actin-associated proteins and some small GTPases that cooperate to regulate actin-based cellular events, such as the formation, elimination, motility, stability, size and shape of dendritic spines [2,6]. This actin cytoskeleton helps explain why a variety of dendritic spines exist, since actin is very dynamic and allows for changes in size and shape of dendritic spines [2].

Additionally, several other organelles can be found within dendritic spines, such as the smooth endoplasmic reticulum, a spine apparatus, clusters of polyribosomes and proteasomes [2,7].

1.1.2. Dendritic spine formation

There are three main views on the origin of dendritic spines which imply different molecular mechanisms of spine origin. The first model states that once dendritic filopodia predominant in younger neurons establish synaptic contact they originate dendritic spines. This model is based on the fact that, as synapses form, the number of filopodia declines and the number of spine-like structures increases, which may suggest that filopodia are the precursors of dendritic spines. So, this model suggests that the highly motile filopodia act as a "probing unit" that searches for appropriate contacts [4]. The axon guidance (suggested by the fact that release of glutamate from sites of presynaptic vesicle release promotes filopodia extension) and cell adhesion molecules present on developing dendrites and axons may contribute to directing the movements of filopodia and their selective adhesion to a compatible axonal partner [4,9].

The second model proposes that dendritic spines arise from synapses that are initially formed on the dendritic shaft. This view is supported from the observation that the majority of synapses in younger pyramidal neurons are located on the dendritic shaft rather than on filopodia [4,10].

The third model states that spines can form even without synaptic contact. Spines of the distal dendritic branches of cerebellar Purkinje neurons form before the establishment of synaptic contact with the presynaptic parallel fibers [4,10].

Since these three models base their assumptions on different types of neurons, it is more likely that dendritic spines emerge through different mechanisms depending on the type of neuron [4]. However, it has also been proposed that these three models might be part of the same process, which occur in specific temporal periods of a neuron's life and may be dependent on the maturation of its dendritic structures (filopodia and dendritic spines) [10].

Following genesis of dendritic spines, they pass through a process of maturation where there is an increase in spine density, a decrease in overall length and a decrease in the number of dendritic filopodia with a simultaneous decrease in spine motility [7]. This maturation process also results in synapse maturation which involves the further recruitment of presynaptic and postsynaptic components (scaffolding proteins and neurotransmitters receptors, for example) [11].

Finally, after maturation of dendritic spines and formed synapses, there is a retraction of some contacts and elimination of inappropriate synaptic proteins, which refine the neuronal circuitry [9], together with long-term potentiation (LTP) and long term depression (LTD) (Figure 3) [11].

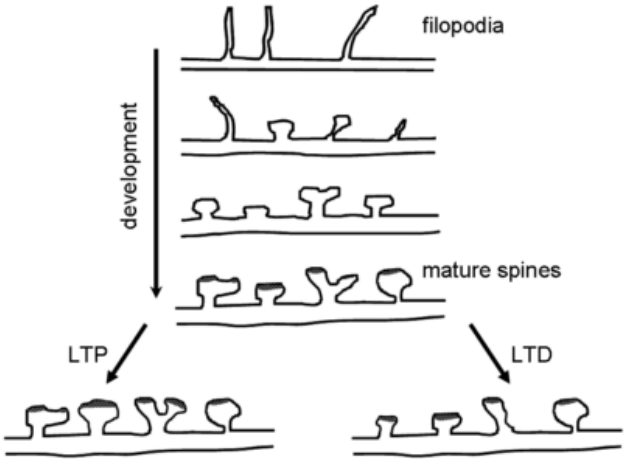

Figure 3 – Dendritic spines development. In the early stages, filopodia begin to differentiate into more mature dendritic spines, which then are refined through LTP or LTD, causing an enlargement or shrinking of the spines, respectively (adapted from [7]).

1.1.3. Dendritic spines and synaptic plasticity

Synaptic plasticity is the ability that neurons have to positively or negatively change the efficacy of their connections in response to neuronal activity [1,2]. This synaptic connectivity is a dynamic entity that is constantly changing in response to neural activity and other influences, and can vary in time from milliseconds to years [1].

Short-term synaptic plasticity includes facilitation, augmentation, potentiation and synaptic depression. Synaptic facilitation is a rapid increase in synaptic strength that occurs when two or more action potentials invade the presynaptic terminal within a few milliseconds of each other. Synaptic augmentation and potentiation are also elicited by repeated synaptic activity and serve to increase the amount of neurotransmitters released from presynaptic to postsynaptic terminals. Synaptic depression opposes facilitation, causing a decline of neurotransmitter release during sustained synaptic activity [1].

Long-term synaptic plasticity includes LTP and LTD [1]. LTP is a long-lasting increase in synaptic strength due to certain patterns of high frequency electrical stimulation, whereas LTD is a long-lasting decrease in synaptic strength due to certain patterns of low frequency electrical stimulation [1,2,4], both of which are thought to be important for memory formation and storage in the brain [5,12]. LTP and LTD are intimately related with the neuronal F-actin cytoskeleton. LTP can result in spine head enlargement accompanied by an increase in F-actin levels, whereas LTD results in shrinkage of dendritic spine heads and even spine elimination which is accompanied with actin depolymerization [2,5,13]. Thus the G-actin/F-actin ratio and all the proteins that can interfere with the former affect the various aspects of dendritic spine morphology and consequently, synaptic plasticity [2].

These enduring forms of synaptic plasticity (LTP and LTD) lead to protein phosphorylation and changes in gene expression which greatly outlast the period of synaptic activity and can yield changes in synaptic strength that persists for hours, days, or even longer. It is an important neural mechanism which modulates several forms of brain plasticity, such as learning new behaviours or acquiring new memories [1].

1.2. Protein Phosphatase 1

Protein phosphatase 1 (PP1) is a Serine/Threonine (Ser/Thr) phosphatase that belongs to the phosphoprotein phosphatase superfamily along with PP2A, PP2B, PP4, PP5, PP6 and PP7 [14,15]. These phosphatases catalyze over 90% of all eukaryotic protein dephosphorylation reactions and among them, PP1 is the most important one in terms of substrate diversity, with close to 200 PP1-interacting proteins (PIPs) have already been identified [15].

PP1 is known to be involved in glycogen metabolism, transcription, protein synthesis, cellular division, meiosis and apoptosis. Additionally, through interaction with its regulatory proteins, PP1 can be involved in neurotransmission, neurite outgrowth and synapse formation [16].

This versatility of PP1 is largely determined by the binding to different specific regulatory subunits, which can function as inhibitors of its activity, substrate-specifying subunits, targeting subunits or substrates. By interacting with its substrates, PP1 can dephosphorylate them at a single or multiple residues, activating or inactivating them. Some proteins can also mediate the targeting of PP1 to specific protein complexes, bringing PP1 in close proximity to specific substrates. PP1 can also interact with proteins which enhance its activity towards a specific substrate, such as myosin phosphatase-targeting subunit 1 (MYPT1). Additionally, some proteins, such as dopamine- and cAMP-regulated neuronal phosphoprotein (DARPP-32) and inhibitors-1/2/3, can directly block PP1 activity, thus inhibiting the dephosphorylation of all PP1 substrates [14–16].

1.2.1. PP1 isoforms

The mammalian genome contains three different genes for PP1 (*PPP1CA, PPP1CB* and *PP1CC*) that encode four distinct catalytic subunits: PP1α, PP1β and the splice variants PP1γ1 and PP1γ2 [14,17].

PP1α, PP1β and PP1γ1 are ubiquitously expressed, while the PP1γ2 isoform is testis-enriched and sperm-specific [17,18]. Even though PP1α, PP1β and PP1γ1 are ubiquitously expressed, their expression levels differ, depending on the cell type and tissue [18,19]. For instance, PP1α is more enriched in the brain (especially in the striatum and hippocampus) and in the heart; PP1β is more enriched in the brain, small intestine, muscle and lung; and PP1γ1 is more enriched in the brain (especially in the striatum and hippocampus), heart and skeletal muscle. Additionally, even in the same cell type, these isoforms have distinct localizations. In neuronal cells, PP1α is specially localized to dendritic spines, PP1β to the soma and dendritic shaft, and PP1γ1 to the dendritic spines and presynaptic terminals [18,20].

1.2.2. PP1 docking motifs

As mentioned above PP1 has nearly 200 validated PIPs, and by using bioinformatics-assisted PIP identification screens it is estimated that hundreds more PIPs remain to be identified and validated. Moreover, PIPs interacts with PP1 in a highly specific manner, forming very stable complexes. This is due to PP1's unique binding motifs, such as RVxF, SILK, MyPhoNE, "SpiDoC", IDoHA, and others [14,15,21].

Among these binding motifs, the RVxF motif is the most common, being present in nearly 70-90% of all validated PIPs. This motif generally conforms to the consensus sequence [K/R][K/R][V/I][x][F/W], with x being any reside other than Phe, Ile, Met, Tyr, Asp or Pro. Interaction between PIPs and PP1 through this motif does not change PP1 conformation and only serves to anchor the PIPs to PP1, bringing them closer to PP1 and promoting secondary interactions that determine the activity and substrate specificity of PP1 [14,15,21] (Figure 4).

The SILK motif, [GS]IL[KR], initially described as being essential for PP1 inhibition by inhibitor-2, is present in seven PIPs and, as the RVxF motif, seems to be essential for PP1 anchoring. The MyPhoNE motif, RxxQ[VIL][KR]x[YW] , is present in seven PIPs and is involved in substrate recognition. Both motifs (SILK and MyPhoNE) are always N-terminal to the RVxF [14,15,21].

"SpiDoC", is a domain in neurabin-2 which binds to the PP1 C-terminal groove, blocking access to substrates that require this groove for PP1 binding, thus directing the substrate specificity of PP1 [15,22]. This domain will be further explained in section 1.3.3.

Aside from the RVxF and the SILK motif, inhibitor-2 has a third motif able to interact with PP1 – IDoHA. This motif binds PP1 in a manner that covers its active site, preventing all PP1 activity [14,15,23].

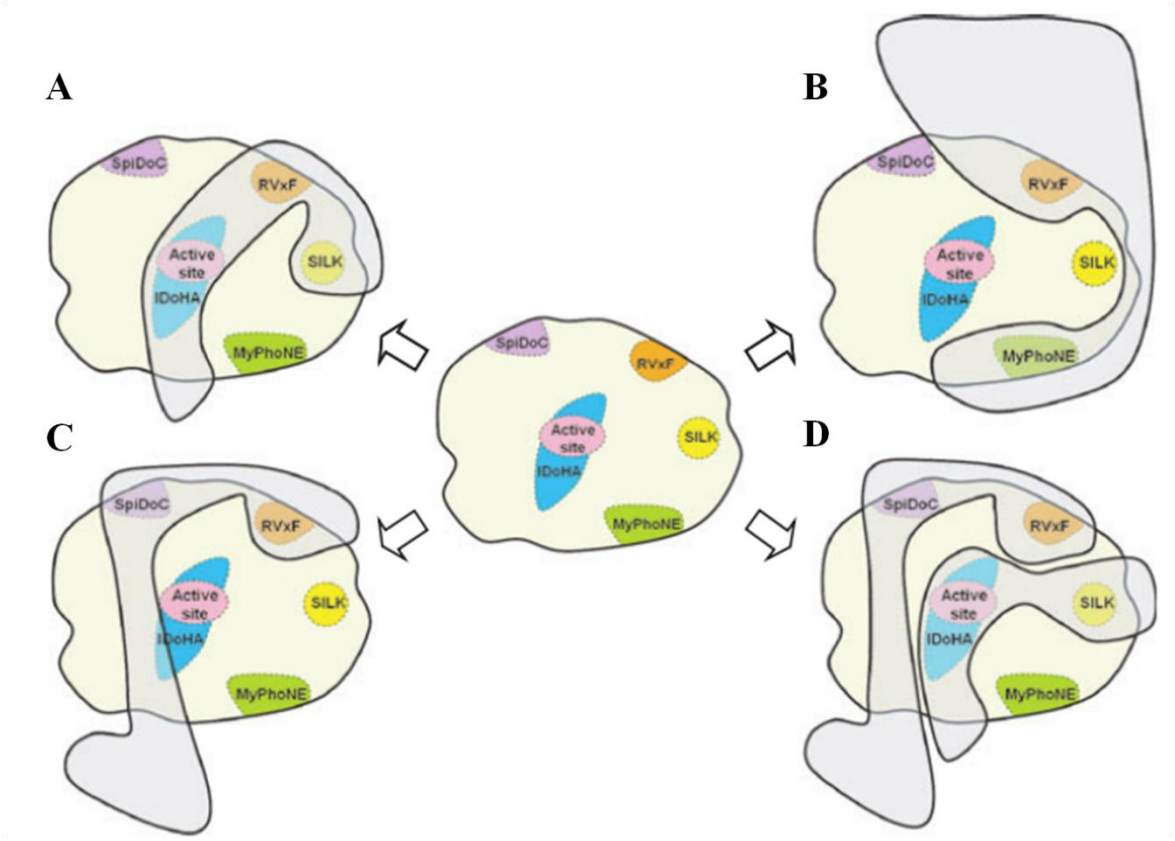

Figure 4 – PP1 docking motifs. PP1 has several surface grooves that bind PIPs docking motifs (middle panel). Several proteins (gray, translucent structure) combine several PP1 docking sites to form unique combinations. Illustrations are based on known structures of PP1 with inhibitor-2 (A), Mypt (B), neurabin-2 (C) and neurabin-2 plus inhibitor-2 (D) (adapted from [15]).

1.3. Neurabins

1.3.1. Neurabin-1

Neurabin-1 is a multifunctional scaffolding protein first identified and characterized in 1997 from purified rat brain tissue [24]. The human neurabin-1 is encoded by the *PPP1R9A* gene (protein phosphatase 1, regulatory subunit 9A) located on chromosome 7 [25] and it is comprised of 1098 amino acids (a.a.) [26]. It has an N-terminal F-actin binding domain (a.a. 1-144), followed by a PP1 binding domain (a.a. 425-502), a PDZ (PSD-95/Dlg/ZO-1) domain (a.a. 504-592), three C-terminal coiled-coil regions (a.a. 597-627, 670-824, 1033-1090) and a sterile alpha motif (SAM) domain (a.a. 988-1051) (Figure 5). These two latter domains are known to mediate homo- and heterodimerization of other proteins. Within the PP1-binding domain it is possible to identify a KIKF motif, conserved in other PP1 regulatory subunits [27]. Neurabin-1 also has some consensus sequences for phosphorylation by several protein kinases [28].

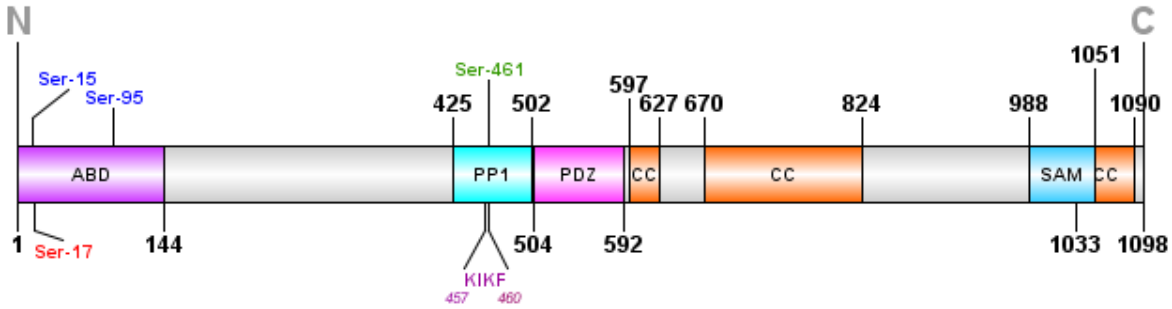

Figure 5 – Neurabin-1 domain structure. Coloured boxes represent the several domains found in neurabin-1. Vertical black lines represent the starting and ending a.a. of the respective domain. KIKF represents the RVxF motif found in neurabin-1. Dark blue, red and green vertical lines represent phosphorylation sites of ERK2, Cdk5 and PKA, respectively. N, N-terminal; C, C-terminal; ABD, F-actin binding domain; PP1, PP1 binding domain; PDZ, PSD-95/Dlg/ZO-1 domain; CC, coiled-coil domain; SAM, sterile alpha motif.

Neurabin-1 is highly concentrated in the synapse and in the growth cone of developed and developing neurons, respectively [24,29]. Initially thought to be neuron-exclusive, neurabin-1 was later found to be expressed both in the brain and skeletal muscle by northern blot [30].

1.3.2. Neurabin-2

Neurabin-2, also known as spinophilin, was initially identified and described in 1997 due to its ability to form a complex with the catalytic subunit of PP1 and due to its potent modulation of PP1 enzymatic activity *in vitro* [31]. In humans it is encoded by the PPP1R9B gene located on the

chromosome 17 and it is comprised of 815 amino acids [32]. It has two F-actin-, a receptor- and a PP1- binding domains, a LIZ and a PDZ domain, and three coiled-coil domains (Figure 6) [32,33].

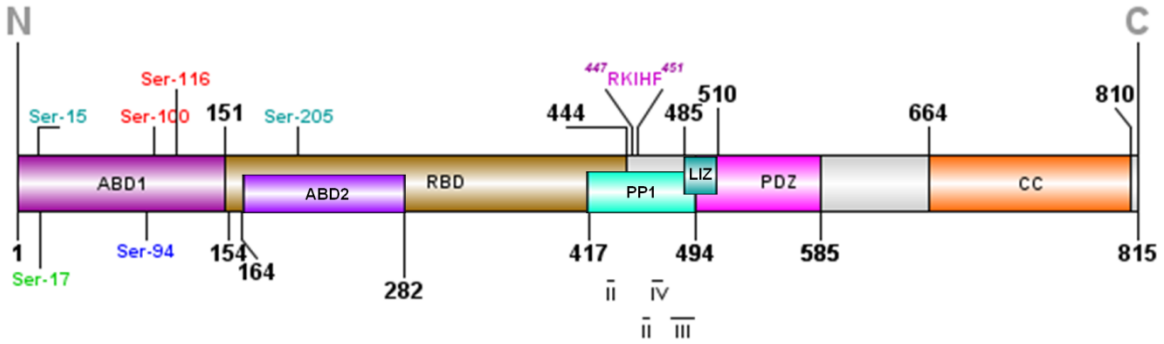

Figure 6 – Neurabin-2 domain structure. Horizontal lines represent the several domains of neurabin-2. Vertical lines represent phosphorylation sites. Light blue, green, dark blue and red represent phosphorylation sites of ERK2, Cdk5, PKA and CaMKII, respectively. RKIHF represents the RVxF motif found in neurabin-2. II, III and IV represent the several additional regions that can bind to PP1. N, N-terminal; C, C-terminal; ABD, F-actin binding domain; RBD, receptor-binding domain; PP1, PP1-binding domain; LIZ, LIZ motif; PDZ, PSD-95/Dlg/ZO-1 domain.

Neurabin-2's F-actin-binding domain, a.a. 1-154, is intrinsically unstructured and upon binding to F-actin adopts a more ordered structure [32,33]. Additionally, a second F-actin binding domain was described between a.a. 164-282. However it is still unknown whether these two domains represent segments of a single domain or two independent domains [33,34].

The receptor-binding domain, located between a.a. 151-444, interacts with the third intracellular loop of various seven transmembrane domain receptors, such as the dopamine D2 receptor and some subtypes of the α-adrenergic and muscarinic-acetylcholine receptors [32,33].

The PP1-binding domain is located within residues 417-494 and contains the pentapeptide RKIHF motif between a.a. 447-451, conserved in other PP1 regulatory subunits [32,33]. Within this domain it is possible to find other regions able to bind to PP1, as it will be described in section 1.3.3 [22].

A LIZ motif was described between a.a. 485-510, known to mediate protein-protein interactions and target protein kinases and protein phosphatases to membrane ion channels. The PDZ domain, a.a. 494-585, directly binds to C-terminal peptides derived from glutamatergic AMPA and NMDA receptors. The three predicted coiled-coil domains between a.a. 664-814 allow for homo- and hetero- dimerization between neurabin-2 and other proteins. Neurabin-2 also has some consensus sequences for phosphorylation by several protein kinases [32,33].

Contrary to neurabin-1, neurabin-2 is ubiquitously expressed. It is highly concentrated in the brain tissue, especially in neurons, where it is enriched in the PSD [35].

1.3.3. Neurabin-1 and neurabin-2 interactome

As scaffolding proteins, both neurabin-1 and neurabin-2 interact with several proteins, dictating their localization within a cell (Table 1and Table 2).

One of the most studied interactions of neurabin-1 and neurabin-2 is their interaction with PP1. The complex formed between neurabin-2 and PP1 is highly unique. Instead of binding to PP1 using only its RVxF motif, neurabin-2 also binds to PP1 in three additional regions: a.a. 430-434 and 456-460 (region II), a.a. 476-492 (region III) and a.a. 462-469 (region IV), with this latter interaction being necessary for directing the substrate specificity of PP1 ("SpiDoC"). Despite this extensive interaction surface, neurabin-2 does not bind PP1 near its active site leaving it unchanged and able to bind to other proteins, which likely explains how neurabin-2 can direct PP1 to a specific substrate, such as the AMPA receptor subunit, GluR1, present on the postsynaptic region of synapses [22]. Ragusa et al., 2010, found that neurabin-1 and neurabin-2 had 100% primary sequence identity in the a.a. required for binding to the PP1 C-terminal groove [22], which suggests neurabin-1 may also interact with PP1 in the same manner as neurabin-2. However, this has not yet been thoroughly investigated.

How neurabin-2 can direct PP1 to a specific substrate has not yet been confirmed, however, a model has been proposed based on the following findings: neurabin-2's PDZ domain is known to bind several proteins, including AMPA and NMDA receptor subunits; when PP1 is bound to neurabin-2, other proteins cannot bind to its PDZ domain, suggesting that neurabin-2 cannot have its PDZ- and PP1-binding domains simultaneously occupied; neurabin-2 is present in dimers, mediated by its coiled-coil domains. Thus, it has been proposed that one molecule of neurabin-2 binds to PP1 through the PP1-binding domain and a second molecule binds to the subunits of the AMPA and NMDA receptors through its PDZ domain. Then, the two neurabin-2 molecules bind each other through their coiled-coil domains, bringing PP1 closer to the receptor, facilitating PP1 dephosphorylation of AMPA and NMDA receptors. The same mechanism has also been proposed for neurabin-1 [36].

Other interactions will not be here fully described as this thesis is not related to them. However, the following tables (Table 1 and Table 2) summarize most of the known interactions between neurabins and other proteins in neurons, and their physiological roles. Neurabin-2 is

ubiquitously expressed and thus, can interact with several proteins not found in neurons [32], which are also not relevant for this thesis. For a more complete list, see Sarrouilhe and Ladeveze, 2014 [32].

Table 1 – Proteins able to interact with neurabin-1 in neurons

Protein	Neurabin-1 motif	Function	References
F-actin	F-actin binding domain	Binds to and binds other proteins to F-actin, regulating neuronal morphology. Promotes bundling and cross-linking of actin fibers.	24,27,37–42
Neurabin-1	Coiled-coil domain	Can form homodimers dictating neurabin-1 effects on cell morphology. May facilitate interaction with other proteins.	27,43–45
Neurabin-2	Coiled-coil domain	Can form heterodimers. Specific function of this interaction has not been yet investigated, but this interaction may negatively regulate neurabin-1/neurabin-2 effects on the neuronal cell.	27,42
PP1α, PP1γ1	RVxF motif	Directs PP1 to F-actin and to specific locations within the cell and regulates its localization and activity. Neurabin-1/PP1 complex regulate synaptic transmission and bidirectional changes in hippocampal plasticity (enhancing LTD and inhibiting LTP), and are important in the formation of filopodia and dendritic spines.	27,38–40,44,46
p70S6k	PDZ domain	Recruits p70S6k to the cytoskeleton at neuronal cell synapses, opposing neurabin-1/PP1 complex in regulating actin rearrangement and cell morphology.	27,37
Kalirin-7	PDZ domain	Regulation of actin cytoskeleton.	47
Rac3	Between a.a. 472-513	Mediates Rac3-induced neuritogenesis by anchoring Rac3 to growth cone F-actin.	48
Lfc	Coiled-coil domain	Recruits Lfc, regulating Rho-dependent organization of F-actin in spines leading to altered spine morphology.	49
TGN38	Coiled-coil domain	May modulate the intracellular trafficking itinerary of TGN38.	45
R4-RGS*, RGS19	Not yet known.	Opposes neurabin-2 binding to R4-RGS and RGS19, removing them from the GPCRs signaling complex and enhancing the intensity of Ca^{2+} signaling.	50
I-2 (IPP-2)	Between a.a. 374-516	Targets the PP1/I2 complex to F-actin, suggesting it regulates cytoskeletal functions and cell morphology.	38
AMPA and NMDA receptor**	PDZ domain	Targets PP1 to these receptors regulating their phosphorylation state and activity.	36

Abbreviations: a.a., amino acids; AMPA, α-amino-3-hydroxy-5-methyl-4-isoxazole propionic acid; I-2 (IPP-2), protein phosphatase inhibitor 2; Lfc, Rho guanine nucleotide exchange factor 2; NMDA, N-methyl-D-aspartate; p70S6k, ribosomal protein S6 kinase beta-1; PP1, protein phosphatase 1; R4-RGS, R4 subfamily of RGS proteins; Rac3, ras-related C3 botulinum toxin substrate 3; RGS, regulators of G protein signaling; TGN38, trans-Golgi network integral membrane protein TGN38.
*Only RGS1, RGS2, RGS4 and RGS16 were tested.
** Subunits GluR2/3 and NR1C2', NR2A/B and NR2C/D.

Table 2 – Proteins able to interact with neurabin-2 in neurons

Protein	Neurabin-2 motif	Function	References
F-actin	F-actin binding domain 1 and 2	Binds along the side of F-actin and has F-actin-cross-linking activity. Directs several proteins to F-actin. It has a central role in actin organization.	34,35,51–54
Neurabin-1	Coiled-coil domain	Can form heterodimers. Specific function has not been yet investigated, but may negatively regulate neurabin-1/neurabin-2 effects on the neuronal cell.	27,42
Neurabin-2	Coiled-coil domain	Can form homodimers, facilitating interaction with other proteins.	45
PP1α, PP1γ1	RVxF, region II, III and IV of the PP1-binding domain	Forms very stable complexes with PP1, targeting it to dendritic spines and directing its substrate specificity.	22
p70S6K*	PDZ domain	Unknown.	55
R4-RGS**, RGS19	Receptor-binding domain	Recruits the RGS protein to the GPCRs signaling complex to reduce the intensity of Ca^{2+} signaling.	50
Dcx	Coiled-coil domain	Enhances Dcx binding to F-actin and facilitates PP1-mediated dephosphorylation of Dcx. Neurabin-2/Dcx complex may be involved in neuronal migration and dendritic spine formation.	56–60
CaMKII	C-terminal domain (non-phosphorylated CaMKII) and between a.a. 151-300 (Thr286-autophosphorylated CaMKII)	Targets CaMKII to F-actin and targets PP1 to CaMKII. This interaction increases with neuronal maturation.	61,62
I-2 (IPP-2)	Between a.a. 354-494	Targets the PP1/I2 complex to F-actin, suggesting it regulates cytoskeletal functions and cell morphology.	38
TGN38	Coiled-coil domain	May modulate the intracellular trafficking itinerary of TGN38.	45
Tiam1	Between a.a. 444-817	Promotes the plasma membrane localization of Tiam1 and enhances its ability to activate p70S6k. Suppresses Tiam1 ability to activate Pak1.	63
3iL of α_{1B}A, α_{2A}A, α_{2B}A and α_{2C}A receptors	Receptor binding domain	Mediates regulation of α_{1B}A receptor Ca^{2+} signaling by RGS2, facilitating interaction of the latter with $G_{\alpha q}$. May also contribute to the localization of these receptors.	64–66
3iL of D2 receptor	Receptor binding domain	May establish a signaling complex for dopaminergic neurotransmission through D2 receptors by linking them to downstream signaling molecules and the actin cytoskeleton.	65,67
M1, M2 and M3 receptors	Receptor binding domain	Seems to recruit these receptors to the cell periphery. Regulates G-protein signaling by forming a complex with these receptors and RGS8.	68,69
3iL of CCKA and CCKB receptor	Not yet identified.	May regulate G-protein signaling by binding to these receptors.	50
AMPA and NMDA receptor***	PDZ domain	Targets PP1 to these receptors regulating their phosphorylation state and activity.	36,70

Protein	Neurabin-2 motif	Function	References
δ- and μ-opioid receptor	Receptor binding domain	Attenuates agonist-driven ERK1/2 phosphorylation mediated upon activation of the δ-opioid receptor, but not on μ-opioid receptor. Modulates δ-opioid receptor signaling in a different manner that that of μ-opioid receptor.	[71]

Abbreviations: 3iL, 3rd intracellular loop; a.a., amino acids; $\alpha_{1/2\text{-A/B/C}}$AR, α-1/2-A/B/C adrenergic receptor; AMPA, α-amino-3-hydroxy-5-methyl-4-isoxazole propionic acid; Ca^{2+}, calcium; CAMKII, Calcium/calmodulin-dependent protein kinase type II; CCKA/B, Cholecystokinin receptor type A/B; D2, D(2) dopamine receptor; DCAMKL1, Serine/threonine-protein kinase DCLK1; Dcx, doublecortin; I-2 (IPP-2), protein phosphatase inhibitor 2; M1/2/3, Muscarinic acetylcholine receptor M1/2/3; NMDA, N-methyl-ᴅ-aspartate; p70S6k, ribosomal protein S6 kinase beta-1; PP1, protein phosphatase 1; R4-RGS, R4 subfamily of RGS proteins; Ras-GRF1, Ras-specific guanine nucleotide-releasing factor 1; RGS, regulators of G protein signaling; Tiam1, T-lymphoma invasion and metastasis-inducing protein 1; TGN38, trans-Golgi network integral membrane protein TGN38.

*_in vitro_ (P.E. Burnett and P.B. Allen, unpublished work).

**Only RGS1, RGS2, RGS4 and RGS16 were tested.

*** Subunits GluR2/3 and NR1C2', NR2A/B and NR2C/D.

1.4. PP1, neurabin-1 and neurabin-2 in dendritic spines

As aforementioned, PP1 is ubiquitously expressed. However, in the brain, more specifically, in neurons, PP1α and PP1γ1 isoforms are highly localized to dendritic spines [18,20]. PP1 has been identified as a key regulator in both LTP and LTD, with PP1 inhibiting LTP while promoting LTD. In fact, LTD-inducing stimuli promotes distribution of PP1 to dendritic spines, where it can dephosphorylate its substrates, such as calcium/calmodulin-dependent protein kinase II (CaMKII), AMPA and NMDA receptors [27,72].

Neurabin-1 is highly concentrated in dendritic spines, even though it can be found in dendrites, axons, terminals and glia. Within dendritic spines, neurabin-1 can be found at high levels in the PSD and the 100 nm subjacent to it. In fact, neurabin-1 concentration falls with increasing distance from the synapse [29]. Neurabin-1 knockout mice exhibited a deficit in contextual fear memory and increased AMPA receptor synaptic transmission, suggesting neurabin-1 regulates LTP [12]. Additionally, neurabin-1 overexpression induced filopodia and dendritic spines [27], further suggesting that it has an important role in spine morphogenesis.

Neurabin-2 is highly enriched at the synaptic membrane in dendritic spines, where it regulates the actin cytoskeleton. Within dendritic spines, neurabin-2 localization is similar to that of neurabin-1. It is predominantly localized in the PSD and the subjacent 100 nm of it, with its concentration decreasing with increasing distance from the synapse [73]. Knockout mice exhibited a marked increase in spine density during development and altered filopodia formation, suggesting it functions as a negative regulator of spine morphogenesis [33,42,52].

Neurabin-1 and neurabin-2 can form hetero- and homodimers and rapidly shuttle on and off the actin cytoskeleton. Through interaction with their respective partners (Table 1 and Table 2), they are able to regulate spine morphology and density, receptor function and synaptic plasticity [38]. They bind an overlapping set of targets with some opposing effects, as can be observed in both Table 1 and Table 2. Also, as beforementioned, neurabin-1 overexpression induced filopodia and dendritic spines [27] while neurabin-2 knockout mice exhibited a marked increase in spine density during development [52]. Additionally, neurabin-1 and neurabin-2 seem to have opposing effects on the regulation of R4-RGS [50,65]. Due to all these opposing effects, it has been proposed that neurabin-1 and neurabin-2 may act as negative regulators of each other, especially in dendritic spines, where they are highly concentrated.

Both neurabins were initially identified as being PP1-targeting subunits. However, between PP1 isoforms, both neurabins showed a significant preference for PP1γ1 and PP1α over PP1β [44].

Since neurabins showed enhanced localization to dendritic spines [29,73], this preference is to be expected, as both PP1γ1 and PP1α are enriched in dendritic spines, while PP1β is more enriched at the neuronal cell body [44].

Disrupting the neurabins/PP1 complex prevents PP1 from reaching some of its targets, thus preventing PP1-mediated dephosphorylation of its substrates. The neurabin-1/PP1 complex is important in the formation of filopodia in young neurons and the transformation of neuronal filopodia into dendritic spines, since it has been shown that disruption of this complex enhances filopodia and impairs surface GluR1 expression, hindering the morphological and functional maturation of dendritic spines [39]. Neurabin-2 targets PP1 to several substrates in dendritic spines (such as AMPA and NMDA receptors), controlling their phosphorylation states [52] and blocking the neurabin-2/PP1 complex prevents PP1-mediated dephosphorylation of the AMPA receptors, decreasing the rundown of AMPA currents and increasing the latter's activity [70].

The neurabins/PP1 complex can be disrupted by phosphorylation. It has been shown that cAMP-dependent protein kinase catalytic subunit alpha (PKA) phosphorylation of neurabin-1 at Ser-461 (near the RVxF site) results in the drastic reduction of PP1 affinity [27,46], allowing neurabin-1 recruitment of other proteins [27]. Even though the RVxF-flanking serine of neurabin-1 is conserved in neurabin-2, PKA does not phosphorylate neurabin-2 at the same site. Instead, it phosphorylates a serine residue in the F-actin binding domain (Ser-94; in rat, PKA can also phosphorylate Ser-177) [16,32,54]. This does not result in reduced PP1 affinity for neurabin-2, but does reduce neurabin-2 interaction with F-actin, displacing neurabin-2 from the PSD to the cytosol, which may ultimately serve to control PP1-mediated changes in the actin cytoskeleton or PP1 anchoring to receptors [54].

Neurabin-1 and neurabin-2 share a conserved site at Ser-17 for cyclin-dependent-like kinase 5 (Cdk5) phosphorylation. However, different research groups reached two different conclusions on neurabin-1 phosphorylation by Cdk5. Futter et. al, 2005 has shown that neurabin-1 can be phosphorylated by Cdk5 at Ser-17 *in vitro* [28], while Causeret et. al, 2007 did not, reporting Cdk5 phosphorylation at Ser-95 instead [74]. This latter research group found that Ser-95 phosphorylation of neurabin-1 affects its ability to bind to F-actin, thus regulating neuronal morphology [74]. As for neurabin-2, Cdk5 phosphorylation at Ser-17 did not affected its ability to bind to F-actin, while extracellular signal-regulated kinase 2 (ERK2) Ser-15 phosphorylation did [28]. This latter kinase can also phosphorylate neurabin-1 at Ser-15, at least *in vitro*. However, the effect of this phosphorylation was not tested [28].

Additionally, neurabin-2 can also be phosphorylated by CaMKII (Ser-100 and Ser-116), which, as with PKA phosphorylation at Ser-94, reduces neurabin-2 ability to bind to F-actin. Neurabin-2 phophorylated at Ser-100 showed enhanced concentration in membrane fractions, including the synaptosomal membrane and synaptic plasma membrane. Both CaMKII and PP1 are enriched in the PSD (with the latter being bound to neurabin-2 which, in turn, is bound to F-actin). CaMKII is autophosphorylated at Thr-286, a critical process for the regulation of synaptic signaling, and PP1 selectively dephosphorylates phospho-Thr-286 CaMKII, preventing its association with NMDA and AMPA receptors. So, CaMKII phosphorylation of neurabin-2 may reduce the interaction between the neurabin-2/PP1 complex with F-actin, thus preventing PP1 from dephosphorylating phospho-Thr-286 CaMKII [62].

Moreover, neurabin-2 localization was shown to vary depending on the kinase that phosphorylates it [28,54,62]. Thus, it has been suggested that phosphorylation of neurabin-2 regulates subcellular localization of the neurabin-2/PP1 complex, targeting this complex to specific locations within dendritic spines [28,62]. Finally, since neurabin-1 can also be phosphorylated by PKA [46], ERK2 and Cdk5 [28,74], but not CaMKII [62], it has been suggested that both neurabin-1 and neurabin-2 scaffolding functions are differentially regulated by phosphorylation [28,62].

Concluding, neurabin-1 and neurabin-2 are scaffolding proteins which can target PP1 (and also other proteins) to different locations within dendritic spines. They seem to act as opposing regulators of each other since they have opposing effects on the actin dynamics of dendritic spines and regulation of R4-RGS. Additionally, their localization, and consequently PP1 localization, changes whether they are phosphorylated or not, which may explain how they can target PP1 to specific substrates within different cellular compartments.

1.5. Alzheimer's disease

Alzheimer's disease (AD) is the commonest neurodegenerative disorder afflicting our older population, contributing to 50-75% of all dementia cases [75,76]. It affects more than 5 million Americans [76,77] and almost 100000 Portuguese [78]. Since our population's average life expectancy is increasing, these numbers are expected to more than double by 2050, making it a major and growing public health concern [76,78].

AD was first characterized in 1907 by Alois Alzheimer, who identified a patient with memory impairment, disorientation both in time and space, and hallucinations. The postmortem examination showed an evenly atrophic brain, the presence of several fibrils and the deposition of a pathological metabolic substance [79].

Since then, our understanding of the pathological lesions associated with this condition improved. However, as of today, there is still no cure and our understanding of the development of this disease still has a lot of gaps which need to be filled [76,80]. Currently, it is known that the core clinical features of AD include gradual and progressive decline in memory, executive function and ability to perform daily activities; however, the disease progresses differently among different individuals [77,81], with some of them showing signs of hallucinations and paranoia while others do not [81]. Histopathologically, AD is characterized by the presence of extracellular amyloid plaques (senile plaques) and intracellular neurofibrilliary tangles [81,82].

Senile plaques are deposits of small peptides – amyloid β peptide (Aβ) – derived via sequential proteolytic cleavages of the amyloid β precursor protein (APP) [83]. Neurofibrilliary tangles comprise paired helical tau filaments, a microtubule binding and stabilizing protein [81]. Aside from these two major changes, AD can also be characterized by neuronal and dendritic loss, neuropil threads, dystrophic neurites, granulovacuolar degeneration, Hirano bodies and cerebrovascular amyloid [82].

1.5.1. AD Forms

There are two forms of AD, the familiar form and the sporadic form, both of which are clinically and histopathologically undistinguishable [84]. The familiar form affects 1% of the patients and has an earlier onset and much more rapid progression than the more common sporadic form [85]. It was the familiar form of AD that brought attention to the Aβ in its pathogenesis since mutations associated with this form were present in the APP gene and in the presenilin genes, PSEN1 and PSEN2. Inheriting any of these mutations guarantees that the individual will develop AD later in

life. The PSEN mutations alter the γ-secretase-mediated proteolytic cleavage of APP, leading to an increase in the production of the more toxic form of Aβ [84,86].

The sporadic form, which accounts for nearly 99% of the cases, is not directly associated with any known mutation and probably involves several different etiopathogenic mechanisms or risk factors [85].

1.5.2. AD risk factors

Advanced age is the greatest risk factor for AD. Additionally, the risk of developing the disease is greater for those individuals who already have a mild cognitive impairment, little to no social and cognitive engagement, moderate to severe brain injury, cardiovascular disease, hypertension, type II diabetes, obesity and dyslipidemia. It is currently unknown whether smoking increases, decreases or has no association with the risk of developing AD [76,86,87].

Aside from the mutations associated with the familiar form of AD, there are other genetic factors that represent a higher risk of developing the disease. To date, the major risk factor described is the ε4 allele of the apolipoprotein E (Apo E) gene (the remaining ε2 and ε3 alleles are protective and neutral, respectively) [76,86,87]. Additionally, mutations in the SORL1, CLU, PICALM, CR1 or BIN1 are also associated with an increased risk of developing AD [86,87].

There are also protective factors associated with AD. Physical activity and consumption of a Mediterranean diet are known protective factors against heart diseases and also improve overall brain health, thus being factors that also decrease the risk of developing AD and other dementias [86,87].

1.5.3. Alzheimer's disease pathology

AD's major hallmarks are, as mentioned above, the presence of extracellular senile plaques and intracellular NFTs. Arising from the existence of these two major changes came two different lines of thought: the first proposes that AD starts with the accumulation of Aβ while the second proposes that it all starts with hyperphosphorylated tau [88]. However, the first hypothesis has been the predominant model to explain the molecular pathogenesis in AD, since it has been found that mutations causing the familiar form of AD result in a similar biochemical phenotype (increased $A\beta_{42}/A\beta_{40}$ ratio) [89]. This hypothesis states that the impaired production of Aβ species, and the subsequent imbalance between Aβ generation and clearance, triggers several events that disrupt neuronal homeostasis (mitochondrial dysfunction, activation of oxidative stress and inflammatory cascades, decreased neuroplasticity, hyperphosphorylation of tau protein and apoptosis). These

events then culminate with neuronal death, and the subsequent clinical features associated with the disease [90].

1.5.4. APP

In mammals, APP belongs to a protein family that includes APP-like protein 1 (APLP1) and 2 (APLP2). It is a type-1 integral membrane protein containing a large extracelullar domain, a hydrophobic transmembrane domain and a short intracellular domain, designated the APP intracellular domain (AICD). APP is encoded by a gene located on chromosome 21 that can undergo alternative splicing generating 8 isoforms, three of which are most common: APP695, APP751 and APP770. APP695 is predominantly expressed in neurons, while APP751 and APP770 are more ubiquitously expressed [91,92]. Unlike all other isoforms, APP695 does not contain a 56 a.a. domain, the Kunitz protease inhibitor (KPI) domain. Some reports have shown that APP isoforms containing the KPI domain are elevated in AD patients and other studies have shown that prolonged activation of NMDA receptor in neurons can shift APP expression from APP695 to KPI-containing APP isoforms which is accompanied by increased Aβ production [83,93].

APP can undergo posttranslational processing via two major pathways: the non-amyloidogenic pathway and the amyloidogenic pathway (Figure 7). In the non-amyloidogenic pathway, APP is initially cleaved by α-secretase, producing a membrane associated C-terminal fragment consisting of 83 a.a. (C83) and a large N-terminal ectodomain fragment (sAPPα) which is released into the extracellular space. C83 is then cleaved by γ-secretase, giving rise to the small peptide P3, and AICD, both of which are quickly degraded [83,89,91,92].

In the amyloidogenic pathway, APP is initially cleaved by β-secretase, which gives rise to a membrane associated C-terminal fragment of 99 a.a. (C99) and sAPPβ, which is released into the extracellular space. C99 is then further cleaved by γ-secretase, releasing AICD and the Aβ peptide [83,89,91,92]. Most of the Aβ produced is the variant of 40 residues ($A\beta_{40}$) but a longer form of 42 residues ($A\beta_{42}$) can also be produced (depending of the γ-secretase exact cleavage site [92]), which is more hydrophobic and thus, more prone to aggregation, being the predominant form present in senile plaques [89].

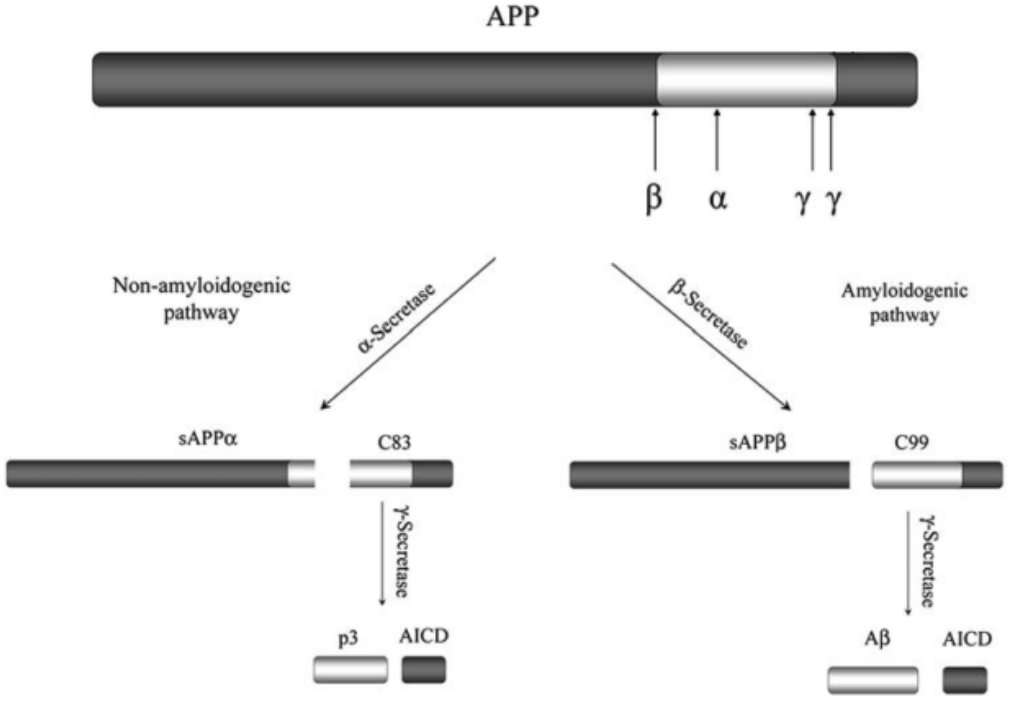

Figure 7 – APP processing. APP can be cleaved by α- or β-secretase, resulting in the secretion of sAPPα or sAPPβ, respectively. The remaining C-terminal fragments, C83 or C99 are further cleaved by γ-secretase, releasing AICD and p3 or Aβ. Depending on the exact site of γ-secretase cleavage the Aβ produced may have 40 ($A\beta_{40}$) or 42 ($A\beta_{42}$) a.a. (adapted from [92]).

APP and its products have important physiological functions. APP is widely accepted as a protein that contributes to cell adhesion via its extracellular domain. The secreted sAPPα has been found to be neuroprotective and is thought to promote neurite outgrowth and synaptogenesis as well as contributing to cell adhesion. sAPPβ only lacks 17 a.a. compared to sAPPα, however it lacks most of the latter's neuroprotective effects. In fact, a study suggested that sAPPβ can be cleaved and stimulate axonal pruning and neuronal cell death. Since AICD is quickly degraded its functions are very difficult to study, however, it has been proposed that it is important in transcription activation and neurite outgrowth [93].

1.5.5. Aβ peptide

AD patients are characterized by the extracellular deposition of insoluble aggregates of the Aβ peptide, which supports the idea that this peptide is essential in the pathogenesis of the disease. However, it was shown that the Aβ peptide in its soluble form is also produced under normal physiological conditions during cellular metabolism. In a healthy brain it is possible to identify different Aβ species ($A\beta_{40}$ and $A\beta_{42}$) at low levels, which suggests they may have important physiological functions [89,94].

It was demonstrated that endogenous Aβ is required for the induction of LTP in the hippocampus as well as for the induction of memory [89,94], and inhibition of Aβ production induces cell death. It was proposed that Aβ could have a negative feedback function preventing excitotoxicity, since it was demonstrated that increased neuronal activity can enhance the production of Aβ which, in turn, depresses synaptic function, decreasing neuronal function [89].

However, despite its possible important physiological roles, Aβ is still widely considered to be the main pathological agent causing AD. Asides from being found in postmortem brains of AD patients, several studies linked Aβ with the major pathological characteristics of this disease, including synaptic toxicity, derangement of the neuronal network and consequently, the progressive memory loss associated with the disease [89,95].

As aforesaid, both soluble $A\beta_{40}$ and $A\beta_{42}$ can be identified even in healthy brains. However, when these peptides form insoluble oligomers they become extremely toxic. $A\beta_{42}$ in particular, is more amyloidogenic and more prone to form aggregates than $A\beta_{40}$ [89,95]. These aggregates were found to block LTP in the hippocampus of rats by binding and cross-linking receptors which are then internalized and degraded in the postsynaptic neuron [94,95]. Particularly, Aβ can lead to synaptic activation of caspase 3 which, in turn, activates calcineurin that dephosphorylates GluR1 subunit of AMPA receptors, leading to their removal from postsynaptic sites [89,95]. These postsynaptic changes lead to a decrease of LTP and/or an increase of LTD, thus leading to an impairment of synaptic plasticity and to a progressive degeneration of synapse [89].

Asides from interfering directly with receptors, Aβ can interfere with mitochondria in neurons. Mitochondrial dysfunction is implicated in AD and several other neurodegenerative diseases and Aβ was found to be within mitochondria in postmortem brains from AD patients. It was found that Aβ induces mitochondrial dysfunction and promotes mitochondrial fragmentation (fission/fusion balance impairment) [89,95], leading to an increased mitochondrial outer membrane permeability and consequently to cytochrome *c* (Cyt *c*) release to the cytosol. Cytosolic Cyt *c* induces the formation of apoptosome and consequent activation of executioner caspases, including caspase 3, which ultimately lead to alterations of basal synaptic transmission, enhancement of LTD, dendritic spine degeneration and behavioral impairment. Additionally, Aβ accumulation may impair the clearance of damaged organelles and proteins (reduced lysosomal degradative efficiency), which results in increased oxidative damage, accumulation of more damaged organelles, decreased adenosine 5'-triphosphate (ATP) production, release of apoptotic factors and, ultimately, neuronal death [89].

2. Aims

AD is a neurodegenerative disorder characterized by a gradual and progressive decline in memory, executive function and ability to perform daily activities. These symptoms are the effect of synaptic loss and ultimately neuronal death, thought to be triggered by the neurotoxicity of Aβ. Thus, studying the proteins involved in the formation and maintenance of dendritic spines (site of the majority of synapses) can help to understand the synaptic loss seen in AD.

The main aim of this thesis was to evaluate the effects of Aβ on two proteins known to be involved in dendritic spine morphogenesis and dynamics (neurabin-1 and neurabin-2) and their interaction with PP1.

The specific objectives were to:

- study the effects of Aβ on the expression of neurabin-1 and neurabin-2;
- evaluate the effects of Aβ on the interaction of neurabin-1 and neurabin-2 with PP1;
- assess the normal cellular distribution of neurabin-1 and neurabin-2 in SH-SY5Y cells;
- evaluate the effects of Aβ on the cellular distribution of neurabin-1 and neurabin-2.

3. Materials and Methods

3.1. Antibodies

Antibodies are a pivotal reagent in many laboratorial techniques. They are host proteins produced in response to the presence of foreign molecules in the body which can recognize a unique part in the foreign molecule - antigen. They have a constant region (Fc) and a variable region (Fab). This latter region binds to a certain epitope of the antigen, which gives each antibody its specificity [96,97].

They can be classified as polyclonal or monoclonal antibodies (Figure 8). Polyclonal antibodies contain multiple clones of antibodies produced to different epitopes on the antigen, while monoclonal antibodies contain a single antibody from one clone of B-cells to a single epitope on the antigen. Thus, polyclonal antibodies are more sensitive, as they can bind to several epitopes giving a larger signal, but are less specific (can bind unspecifically to other proteins that share the same epitope) than monoclonal antibodies, which are highly specific but less sensitive [96,97].

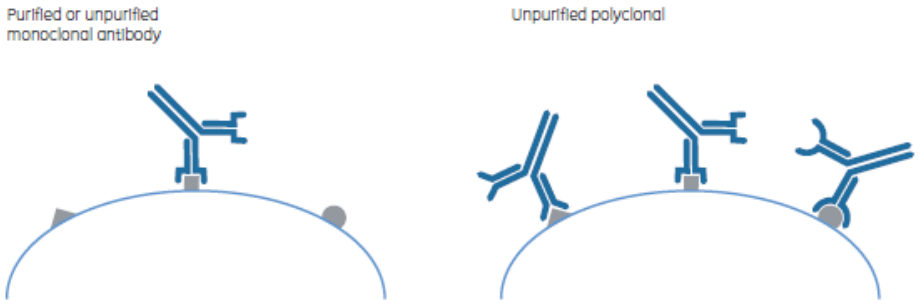

Figure 8 – Monoclonal and polyclonal antibodies. Monoclonal antibodies (left) can only bind to a specific epitope, while polyclonal antibodies (right) can bind to several different epitopes (adapted from [97]).

The following tables (Table 3 and Table 4) summarize the different antibodies used in this thesis.

Table 3 – Primary antibodies and specific dilutions used

Antibody	Antibody type	Target	Dilution
Anti-Neurabin-I (D-4) (Santa Cruz Biotechnology, Inc.)	Mouse, polyclonal	Neurabin-1	WB: 1:100 ICC: 1:50
Anti-PPP1R9B (Proteintech)	Rabbit, polyclonal	Neurabin-2	WB: 1:1000 ICC: 1:100
Anti-PP1α (CBC2C)[19]	Rabbit, polyclonal	PP1α	WB: 1:2500 ICC: 1:250 Co-IP: 4 µl/1000 µg
Anti-PP1γ (CBC3C)[19]	Rabbit, polyclonal	PP1γ	WB: 1:5000 ICC: 1:500 Co-IP: 3 µl/1000 µg
Anti-β3-tubulin (Millipore)	Mouse, monoclonal	β3-tubulin	WB: 1:1000
Anti-MAP2 (Calbiochem)	Mouse, monoclonal	MAP2	WB: 1:500

Abbreviations: Co-IP, co-immunoprecipitation; ICC, immunocytochemistry; WB, western blot

Table 4 – Secondary antibodies used

Antibody	Target	Dilution
Horseradish peroxidase-conjugated anti-mouse (Amersham Pharmacia)	Anti-mouse primary antibodies	1:5000
Horseradish peroxidase-conjugated anti-rabbit (Amersham Pharmacia)	Anti-rabbit primary antibodies	1:5000

3.2. Cell culture

3.2.1. Culture, growth and maintenance of SH-SY5Y cell line

The SH-SY5Y neuroblastoma cell line was chosen since it is human derived and can be differentiated to a more mature neuronal-like phenotype. Originally derived from a metastatic bone tumor biopsy, SH-SY5Y cells are a subline of the parental line SK-N-SH, which were subcloned three times: first to SH-SY, then to SH-SY5, and finally to SH-SY5Y [98].

SH-SY5Y cells (ATCC® CRL-2266™) were grown and maintained in Minimal Essential Medium (MEM)/F12 (1:1) medium supplemented with 10% fetal bovine serum (FBS), 0.5 mM L-glutamine, 100 U/mL penicillin and 100 mg/mL streptomycin. Cultures were maintained at 37°C under 5% CO_2. Cells were subcultured whenever 80-90% confluence was reached.

3.2.2. Differentiation of the SH-SY5Y cell line

SH-SY5Y can be differentiated into a more mature, neuronal-like phenotype through the addition of several different compounds into their medium. One of the most commonly used and best characterized methods for induction of differentiation in SH-SY5Y cells, is the addition of retinoic acid (RA) to the culture medium. RA is a vitamin A derivative known to possess growth-inhibiting and cellular differentiation-promoting properties. Usually, RA is administered at a concentration of 10 μM in serum-free or low serum medium to induce differentiation. However, it is possible to find in the literature several variations of this differentiation medium, with some research groups using medium with different concentrations of serum and/or by administering RA for different number of days [98]. Due to all of these variations, it was decided to test several different combinations of FBS and RA in the media in order to optimize the differentiation parameters, as depicted in Table 5.

Table 5 – Different combinations of FBS and RA used in the experiments

Media	FBS (%)	RA (μM)
A	10	10
B	10	20
C	3	10
D	3	20
E	1	10

Abbreviations: FBS, fetal bovine serum; RA, retinoic acid

All the remaining constituents of the media are the same as described in section 3.2.1. SH-SY5Y cells were differentiated with these different combinations of FBS and RA for 10 days, with the media being renewed every 2 days.

To confirm whether the tested conditions were capable of inducing differentiation, controls were grown in the same media without the addition of RA.

3.2.3. Culture, growth and maintenance of rat primary cultures

Experiments were also carried out in rat primary hippocampal cultures, provided by a laboratory colleague. The hippocampus was dissected from Wistar Hannover rat embryo at 18th day of gestation and dissociated with trypsin (2.25 mg/mL) and deoxyribunoclease I (1.5 mg/mL) in Hank's Balanced Salt Solution (HBSS) for 5 minutes at 37°C. Cells were washed with HBSS supplemented with 10% FBS to stop trypsinization, centrifuged at 1000 rpm for 2 minutes, and further washed and centrifuged with HBSS for serum withdraw. Cells were plated onto poli-D-lysine coated dishes at a density of $1.0x10^5$ and cultured for 10 days in Neurobasal medium (Gibco) supplemented with 2% B27 (Gibco), a serum-free medium combination. The medium was further supplemented with glutamine (0.5 mM), gentamicin (60 μg/mL), and glutamante (25 μM). Cells were maintained in an atmosphere of 5% CO_2 at 37°C and observed in an inverted optical microscope. Five days after plating, 25% of culture medium was replaced with glutamate-free complete Neurobasal medium. After 10 days in culture, cells were used for experimental procedures.

3.2.4. Aβ treatment of SH-SY5Y cell line and rat primary cultures

To evaluate the effects of Aβ on the expression and interaction of several proteins, differentiated SH-SY5Y cells and rat primary hippocampal cultures were incubated with different concentrations of Aβ peptide for 24 hours.

Synthetic $Aβ_{1-42}$ (American Peptide) was dissolved in water to prepare 1 mM stock solutions. Exposure of cells to these Aβ peptides was preceded by an aggregation step, which was achieved by incubating the peptides for 48 hours at 37°C with phosphate buffered saline (PBS) 1x at concentration of 100 μM [99].

SH-SY5Y cells were incubated for 2 days with media E (Table 5) and then incubated for 24 hours in serum free Minimal Essential Medium (MEM)/F12 (1:1) medium supplemented with 0.5 mM L-glutamine, 100 U/mL penicillin, 100 mg/mL streptomycin and 10 μM RA with different $Aβ_{1-42}$ peptide concentrations: 2 μM $Aβ_{1-42}$ and 10 μM $Aβ_{1-42}$. Prior to $Aβ_{1-42}$ treatment, cells were washed twice with PBS 1x.

Rat primary hippocampal cultures were plated as described in section 3.2.3 and washed twice before treatments. Cells were incubated with 2 μM $Aβ_{1-42}$ and 10 μM $Aβ_{1-42}$ for 24 hours in a B27-free Neurobasal medium combination.

Control cultures in both cell lines received PBS 1x vehicle. This was to ensure that the results obtained were not due to the PBS, which was used to aggregate the $A\beta_{1-42}$ peptide, but due to the peptide itself.

3.2.5. Cell Collection and Protein Quantification

Cells were collected using different methods depending on the experimental procedure.

To analyze protein expression, cells were collected using 140 µl of sodium dodecyl sulfate (SDS) 1%. SDS is a strong ionic detergent, able to solubilize lipids and proteins in the membrane of cells, creating pores within the membrane and eventually leading to full cell lysis [97].The resulting lysates were subjected to western blot analysis.

For the purpose of testing protein interactions through co-immunoprecipitation (Co-IP), cells were collected using lysis buffer (50 mM Tris-HCl pH 8.0, 120 mM NaCl, 4% CHAPS) containing protease inhibitors (0.5 mM PMSF, 1 mM Benzamidine, 10 µM Leupeptin, 20 µg/mL Aprotinin, 1 µM Pepstatin A, 1 mM Sodium Fluoride, 1 mM Sodium Orthovanadate), to prevent proteolysis, dephosphorylation and denaturation of proteins.

Following cell collection and protein extraction, protein concentration of each sample was assessed through Pierce's bicinchoninic acid (BCA) protein assay kit (Thermo Scientific) following the manufacturer's instructions. This assay combines the reduction of Cu^{2+} to Cu^{1+} by protein in an alkaline medium with the highly sensitive and selective colorimetric detection of Cu^{1+} by bicinchoninic acid [100]. This procedure was performed in a 96-well plate for spectrophotometric analysis. Standard samples were prepared using known amounts of bovine serum albumin (BSA), as depicted in Table 6. The remaining samples were prepared by mixing 5 µL of the cell lysate with 20 µL of 1% SDS. Following preparation of the samples, 200 µL of working reagent was added to each well. The working reagent was prepared by mixing BCA reagent A with the BCA reagent B in a 50:1 proportion. The 96-well plate was then incubated for 30 minutes at 37°C, after which the absorbance was measured at 562 nm using a microplate reader (Infinite M200, Tecan). A standard curve was obtained by plotting standard absorbance vs BSA concentration, and used to determine the total protein concentration of each sample.

Duplicates of all samples were assayed by this method.

Table 6 – Protein standards used in BCA Protein Assay method

Standard	BSA (µL)	1% SDS (µL)	Protein Mass (µg)
P0	0	25	0
P1	1	24	2
P2	2	23	4
P3	5	20	10
P4	10	15	20
P5	20	5	40

Abbreviations: BCA, bicinchoninic acid; BSA, Bovine Serum Albumin; SDS, Sodium Dodecyl Sulfate

3.3. Co-immunoprecipitation

To test whether Aβ influences the interaction between PP1 (both α and γ isoforms) and neurabin-1 and neurabin-2, a co-immunoprepitation (Co-IP) was performed using SH-SY5Y cells. This technique is a variant of immunoprecipitation and relies on the immunodepletion of a protein of interest ("bait") together with all its protein interacting partners ("prey") in solution [101].

In the experimental procedure the Co-IP was carried out using Dynabeads® Protein G (Invitrogen) because magnetic bead-based separation is rapid and easy to perform, allows for gentle separation which preserves most protein-protein interactions, and significantly reduces background caused by non-specific binding. The procedure is based on the ability of Dynabeads® Protein G to bind to a primary antibody through their Fc region [102]. These antibody-bound magnetic beads are then placed on a Dynal magnet, which causes these beads to migrate to the side of the tube facing the magnet, allowing for easy removal of the supernatant. A sample of proteins is then added to these magnetic beads which permits that the bait in the sample, and consequently any bait-prey complex, bind to the antibody-bound magnetic beads. Then, by using the Dynal magnet and removing the supernatant, only the bait-prey complex is left, which can then be analyzed [101,102]. In the experimental procedure here used, this complex was analyzed through SDS-polyacrylamide gel electrophoresis (SDS-PAGE).

Cell culture was performed as described in section 3.2.4 in 100 mm culture dishes with media E (Table 5). Following 24 hours of Aβ treatment, media were removed, cells were washed with cold PBS 1x and then gently scrapped off the culture plate with lysis buffer (50 mM Tris-HCl pH 8, 120 mM NaCl, 4% CHAPS) containing protease inhibitors (0.5 mM PMSF, 1 mM Benzamidine, 10 µM Leupeptin, 20 µg/mL Aprotinin, 1 µM Pepstatin A, 1 mM Sodium Fluoride, 1 mM Sodium Orthovanadate). Lysates were collected and then sonicated twice for 10 seconds.

Each sample had its mass normalized using the BCA assay described in section 3.2.5 and 1000 μg of each was then precleared with 15 μL Dynabeads for 1 hour at 4°C with agitation. In a separate microtube, 40 μL of Dynabeads were added to 200 μL of washing solution (to ensure proper agitation) with the primary antibody (PP1α and PP1γ at respective dilutions, depicted in Table 3) for 1 hour at 4°C with agitation. Prior to use, Dynabeads were washed thrice with washing solution (3% BSA/PBS) and then stored at 4°C.

After 1 hour, each sample was transferred to the antibody-containing microtube, previously washed with 200 μL of washing solution, and were then incubated overnight at 4°C with agitation. Following the incubation period, the supernatant was removed and the beads washed thrice with 500 μL of PBS 1x for 10 minutes at 4°C with agitation. After the last wash, the supernatant was fully discarded and the beads resuspended in 100 μL of 1x Loading Buffer (LB) and boiled for 10 minutes at 90°C for disruption of the Dynabead-proteins complex. Dybabeads were removed and samples were stored at -20°C until needed.

Co-IP controls were performed by incubating cell extracts with Dynabeads without antibody.

3.4. Western Blot

Western blot (WB), also known as immunoblot, is a widely used technique for the detection and analysis of proteins. It involves several steps which allow for the detection and analysis of the protein of interest. Initially, samples need to be prepared, then separated on an electrophoresis gel and finally transferred onto a nitrocellulose membrane. After transfer, membranes are incubated with antibodies, detected and finally analyzed [97].

In the present work electrophoresis gels were 5-20% gradient SDS-PAGE, a denaturing gel, which allows for separation of proteins solely on the basis of their molecular weight. It consists of two gels, a resolving (bottom), with higher concentration of polyacrylamide to separate proteins, and a stacking (top) gel, with lower concentration of polyacrylamide [97].

Prior to loading the samples, a loading buffer is added, which consists of glycerol, SDS, a reducing agent (β-mercaptoethanol) and a dye (bromophenol blue). Glycerol increases density to the samples and helps anchor the sample in the wells; SDS masks any inherent charge of the proteins; the reducing agent breaks any disulfide bonds, disrupting quaternary and tertiary protein structures; and the dye enables tracking of the progression of the sample in the gel [97].

Electrical current is then applied to the gel, enabling the separation of proteins. After separation, the proteins are transferred electrophoretically onto a nitrocellulose membrane. This

immobilized all proteins that were initially loaded into the gel, at their respective relative migration positions at the time point when the electric current of the gel run was stopped [97].

Following transfer, membranes can be stained with Ponceau S to confirm whether the proteins were transferred and assess equal gel loading. Membranes are then blocked with non-fat dry milk or BSA to block any non-specific binding sites of the primary antibody. After blocking, membranes are incubated with a specific primary antibody and the appropriate secondary antibody. Following incubation, proteins can be detected through chemiluminescence, a method that incorporates the ability of the horseradish peroxidase conjugated on the secondary antibody to catalyze the oxidation of luminol, resulting in the emission of light. This light signal can then be detected on X-ray film which can be analyzed in a densitometer [97].

In the present work, samples were collected and their protein concentration determined as described in section 3.2.5. Samples were separated on a 5-20% gradient SDS-PAGE in a Hoefer electrophoresis system. The gradient gels were prepared and allowed to polymerize for 45 minutes at room temperature. Subsequently, the stacking gel solution was prepared and loaded on the top of the resolving gel. A comb was inserted into the stacking gel and left to polymerize for 30 minutes at room temperature. Prior to loading, LB 4x was added to the samples (1/4 of the final volume), boiled for 10 minutes at 90°C and spun down.

Samples were gently loaded into the wells as well as a molecular weight marker (Precision Plus Protein™ Dual Color Standards, Bio-Rad) and gels were run at 90 mA for approximately 3 hours. Proteins were then electrophoretically transferred onto nitrocellulose membranes (Whatman®) for 18 hours at 200 mA. Membranes were incubated with Ponceau S solution for 5 minutes and scanned in a GS-800 calibrated imaging densitometer (Bio-Rad), in order to assess equal gel loading. Following washing in TSB-T 1x to remove the Ponceau S staining, membranes were blocked with 5% BSA in Tris Buffered Saline Tween (TBS-T) 1x for 4 hours. Membranes were then washed in TBS-T 1x for 10 minutes, incubated with a specific primary antibody (depicted in Table 3) overnight, washed thrice with TBS-T 1x for 10 minutes each, incubated with the appropriate secondary antibody for 2 hours and washed thrice with TBS-T 1x for 10 minutes. Following the last wash, membranes were incubated with enhanced chemiluminescence (ECL) detection kit for 1 minute or with Luminata™ Crescendo Western HRP Substrate (GE Healthcare) for 5 minutes, in a dark room. After exposure of the membranes to X-ray films (Kodak), these were developed and fixed with the appropriate solutions (Kodak). Films were then scanned in a GS-800 calibrated imaging densitometer (Bio-Rad) and the results analyzed.

3.5. Immunocytochemistry

Immunocytochemistry is a technique that permits the visualization of the localization of a specific protein in animal cells and tissues fixed in paraformaldehyde (PFA) [96].

Initially, samples are prepared by fixing with a fixation agent, which helps to stabilize and preserve cells as close to life-like as possible by binding to reactive groups on proteins and lipids in the cells and holding them in the same position as if they were in living cells. Then cells are permeabilized so that antibodies penetrated inside fixed cells. This is achieved by the addition of detergents, which can solubilize membranes without destroying protein-protein interactions. Following permeabilization, cells are blocked, incubated with the proper specific antibody and appropriated fluorescent secondary antibody and mounted on a microscope slide. Cells are mounted in a media with anti-fading and anti-photobleaching properties. Subsequently preparation can be visualized through a microscope and the images analyzed [96].

In the present work, cell culture was performed as described in 3.2.4 in 24-well plates (Corning) with coverslips. Cells were then washed with PBS 1x and 300 µL of 4% PFA was added for 20 minutes. Following fixation, cells were washed trice with PBS 1x and 300 µL of 0.2% Triton-X was added for 10 minutes. Cells were then incubated for 2 hours with the specific antibodies, as depicted in Table 3, followed by incubation for 1 hour with the appropriate fluorescent antibodies (Table 7). Cells were washed thrice with PBS 1x following permeabilization with 0.2% Triton-X, between antibody incubation periods and after incubation with the secondary antibodies. Samples were then mounted on a microscope slide with VECTASHIELD® Mounting Media with DAPI (Vector Laboratories) and visualized using a LSM510-Meta confocal microscope (Zeiss) and a 63x/1.4 oil immersion objective. The argon laser lines of 405 nm, 488 nm, and a 561 nm DPSS laser were used. Profiles were acquired using the Zeiss LSM 510 4.0 software.

Table 7 – Secondary antibodies used in immunocytochemistry

Antibody	Excitation maximum (nm)	Emission maximum (nm)	Observed colour
Alexa Fluor 594 goat anti-mouse IgG (Invitrogen)	590	617	Red
Alexa Fluor 488 goat anti-rabbit IgG (Invitrogen)	495	519	Green

Following image acquisition, co-localization analysis was performed to assess whether Aβ would affect the co-localization between neurabin-1 and both PP1s. Co-localization is occasionally used to estimate the interaction between different molecules, i.e., if different proteins interact with each other. However, when two proteins co-localize, it does not imply that these interact with each other but it supports a physical interaction *in vivo* [103].

The co-localization analysis was performed in the Fiji image processing package, using the JACoP plugin. This plugin uses several pixel intensity spatial correlation methods to determine colocalization between two different colour channels, such as the Manders, the Costes, the Pearson or the Li methods. In the work here described, results were obtained using the Manders' method, since it is normally the most used when comparing two objects of different amounts (in this case two proteins which have different expression levels) [103,104].

Co-localization of PP1α and neurabin-1 was analyzed using 79 and 101 cells for controls and cells treated with $A\beta_{1-42}$, respectively. For the PP1γ and neurabin-1 analysis, 91 and 85 cells were analyzed for controls and cells treated with $A\beta_{1-42}$, respectively. Finally, for the neurabin-2 and neurabin-1 analysis, 62 and 59 cells were analyzed for controls and cells treated with $A\beta_{1-42}$, respectively.

4. Results & Discussion

4.1. Differentiation of the SH-SY5Y cell line

In order to use a cell line closer to neurons, an experiment design was delineated so as to optimize the best media combination for SH-SY5Y differentiation. Initial plating density was of $1x10^5$ per well and cells were allowed to differentiate for 10 days, with media renewal every 2 days. Every 2 days, photographs were taken and those cells collected for further WB analysis.

SH-SY5Y cells are often used in neuroscience due to their ability to differentiate in a more mature neuron-like phenotype. SH-SY5Y cells generally have two morphologically distinct types: "S" and "N". The "S"-type is more epithelial-like with no processes, whereas the "N"-type is more neuronal-like with pyramidal bodies and long processes. "S"-type cells generally do not differentiate and can even begin to replicate indefinitely even when RA, which has growth-inhibition properties, is added to the media. So, an optimized differentiation media should be able to tip the balance in favor of the "N"-type population [98].

To evaluate whether SH-SY5Y cells were differentiated, we decided to look at important characteristics: morphological changes, such as neurite extension, and the expression of neuronal markers, such as the increase in β3-tubulin and microtubule-associated protein 2 (MAP2) [98,105]. Additionally, the presence of "S"-type cells was also evaluated.

4.1.1. Morphological evaluation

To evaluate the morphological changes induced by each media, photographs of cells were taken, in every type of media, every 2 days, depicted in the following images (Figure 9, Figure 10 and Figure 11). No photographs were taken of media E at the 4th, 6th and 8th day due to a technical issue in the camera.

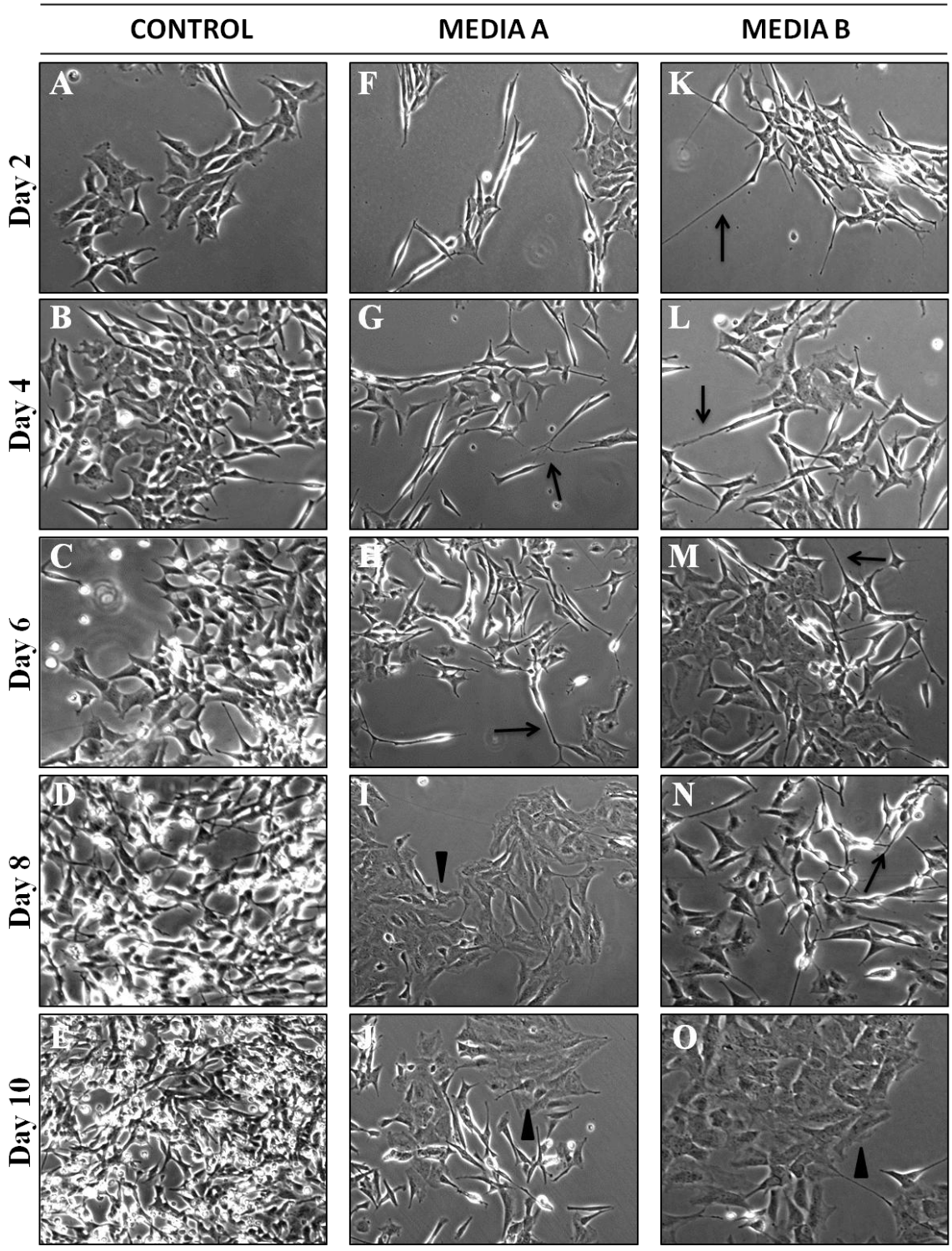

Figure 9 – Phase contrast photographs of SH-SY5Y cells grown in media A and B. A-E represents control cells at days 2, 4, 6, 8 and 10, in this order; F-J represents differentiated cells grown in media A at days 2, 4, 6, 8 and 10, in this order. K-O represents differentiated cells grown in media B at days 2, 4, 6, 8 and 10, in this order. Black arrows represent extended neurites. Black triangles represent "S" population.

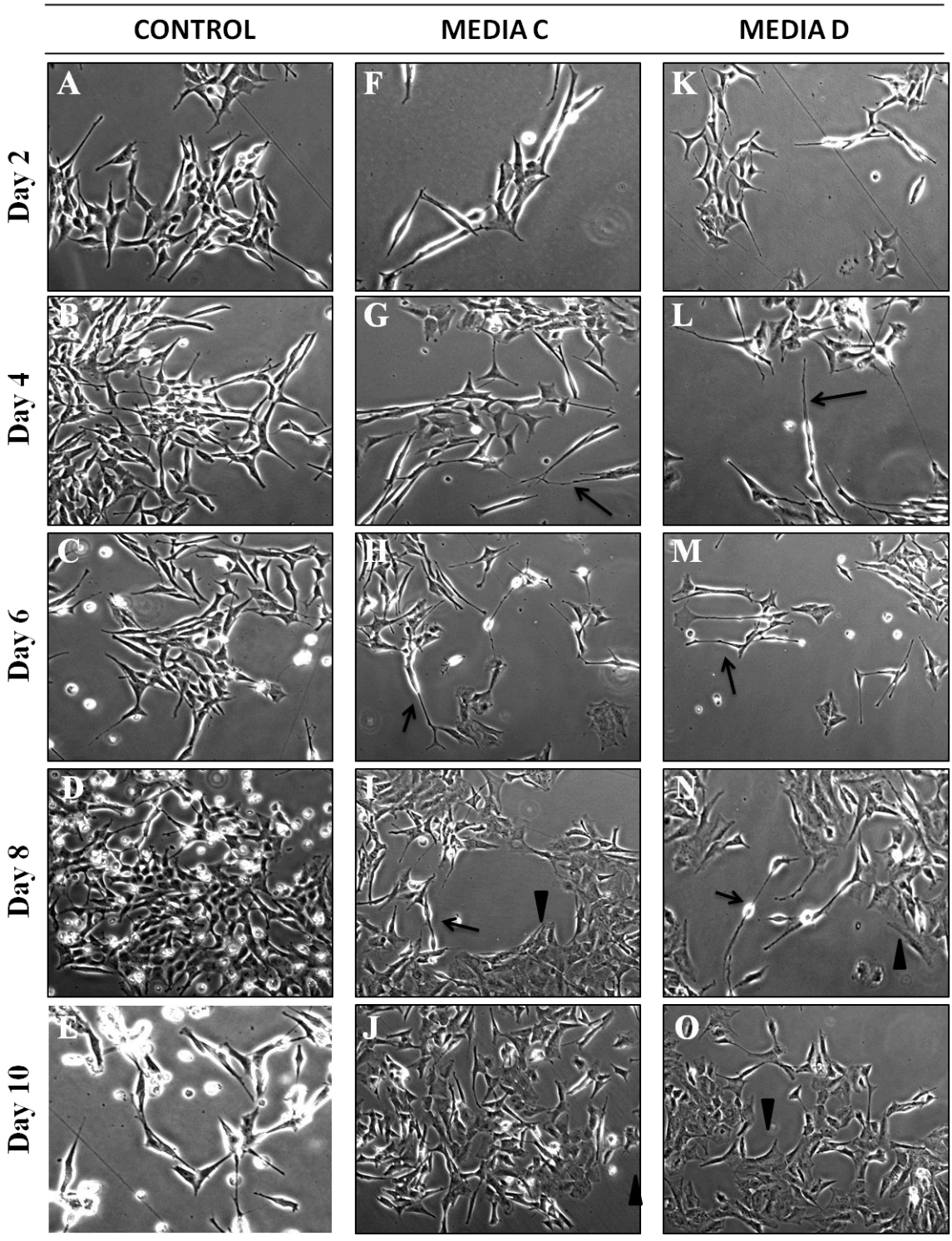

Figure 10 – Phase contrast photographs of SH-SY5Y cells grown in media C and D. A-E represents control cells at days 2, 4, 6, 8 and 10, in this order; F-J represents differentiated cells grown in media C at days 2, 4, 6, 8 and 10, in this order. K-O represents differentiated cells grown in media D at days 2, 4, 6, 8 and 10, in this order. Black arrows represent extended neurites. Black triangles represent "S" population.

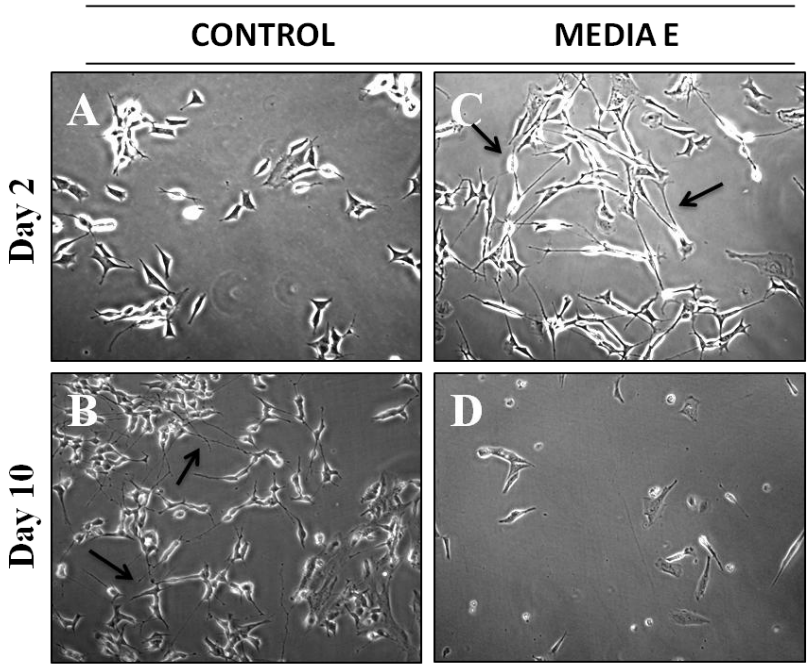

Figure 11 – Phase contrast photographs of SH-SY5Y cells grown in media E. A and B represent control cells at day 2 and 10, respectively; C and D represent differentiated cells at day 2 and 10, respectively. Black arrows represent extended neurites.

The following table summarizes the different morphological changes induced by each different media. Even though no photos were taken of media E at the 4th, 6th and 8th days, the morphological analysis was still carried out.

Table 8 – SH-SY5Y morphological changes induced by the media

Media	Day	Neurite extension	Proliferation rate	"S" population
A	2	+/-	+	-
	4	+	++	-
	6	+/-	++	+
	8	-	++	+
	10	-	++	+
B	2	+	+	-
	4	+	++	-
	6	+/-	++	+/-
	8	-	++	+
	10	-	++	++
C	2	+/-	-	-
	4	+	-	-
	6	+	+	+/-
	8	+/-	+	+
	10	+/-	+	+
D	2	+	-	-
	4	+	-	-
	6	+	+	+/-
	8	+/-	+	+
	10	+/-	+	+
E	2	++	-	-
	4	++	--	-
	6	n/a	n/a	n/a
	8	n/a	n/a	n/a
	10	n/a	n/a	n/a

+, increased; ++, more increased; +/-, neither increased nor decreased; -, decreased; --, more decreased; n/a, almost no cell was available for proper evaluation.

From the results summarized in Table 8, it was possible to observe that cells grown in media A and B had an increased proliferative rate, with the number of cells increasing rapidly each 2 days (Figure 9). Cells grown in media C and D showed a decreased proliferative rate in the initial days, however, their number began to increase rapidly from the 6th day onward (Figure 10). As for cells grown in media E, they began to die between the 4th and 6th days, with almost no cells left in the 10th day (Figure 11B).

Neurite extension was higher in cells grown in media C, D and E than cells grown in media A and B. By comparing media C, D and E, it is possible to observe more developed neurites in the latter, while C and D did not exhibit significant differences between them.

The "S" population increased in all media beginning at the 6th day (media E excluded). By the 10th day, all cultures were overgrown by this type of population, with almost no "N"-type cell left.

It is known that RA has growth-inhibition properties [98]. Thus, when added to the media, SH-SY5Y cells should choose to differentiate rather than divide. However, cells grown in media with high serum concentration (media A and B) preferred to divide. Contrarily, cells grown in media with low serum concentration (media E) chose to differentiate, eventually dying between the 4th and 6th days. This was probably due to RA's toxic effects and low FBS concentration, as FBS provides cells growth factors, hormones, fatty-acids, vitamins and other proteins, necessary for their survival [106]. Controls of media A-D also have shown this fact. Control cells of media A and B divided continuously, and in the 8th and 10th days they were so high in number that eventually started entering apoptosis, probably due to lack of space, which SH-SY5Y require to proliferate [98].

One common aspect to all types of media was the fact that "S"-type cells began to appear at the 6th day and eventually, cultures were overgrown by this type of cells. As can be seen in Figure 9 and Figure 10 (black triangles), "S"-type cells do not have neurites, tend to grow in clusters and have a more epithelial-like phenotype. This aspect has been documented before, with short term RA treatment appearing to induce differentiation of the "N"-type population, while longer treatments promoted proliferation of the "S"-type population, thus resulting in an unbalanced proportion between both populations [98]. As a result of this observation, it was concluded that the differentiating media that would be chosen could only be used on SH-SY5Y cells up to 4 days.

No significant morphological differences were seen between media C and D. It was concluded that either concentration of RA (10 or 20 μM) appeared to have the same results in the morphological changes of SH-SY5Y cells.

Controls of all types of media also have shown an interesting aspect. By observing all control conditions, it is possible to observe that by only reducing the serum concentration of media, SH-SY5Y cells began to develop more extended neurites. Controls of media A and B (Figure 9, A-E) showed that cells with higher concentration of serum in the media prefer to divide and proliferate, almost exclusively. However cells with lower concentration of serum began to develop neurites, as can be seen in Figure 10 (A-E) and Figure 11 (A, B). In the latter this change is more prominent, with cells at the 10th day having developed neurites almost as extended as cells grown in media C and D. This is probably due to the fact that the media has low levels of FBS, thus almost no growth factor [106]. Since there is almost no growth factor in the media, cells could not divide and proliferate but did differentiate.

Thus, by analyzing this data, it is possible to conclude that media C, D and E induced more neuronal-like morphological changes than media A and B. Media C and D had no significant

changes between them at the morphological level, and media E lead to cell apoptosis when used for more than 4 days.

4.1.2. Neuronal markers analysis

Since morphological evaluation of SH-SY5Y cells is not sufficient to conclude whether a population is differentiated or not, WB analysis was carried out to detect the levels of two proteins commonly used as neuronal markers, β3-tubulin and MAP2 [98]. With the results obtained from the morphological evaluation, WB analysis was performed for media C, D and E. The following images summarize the results obtained.

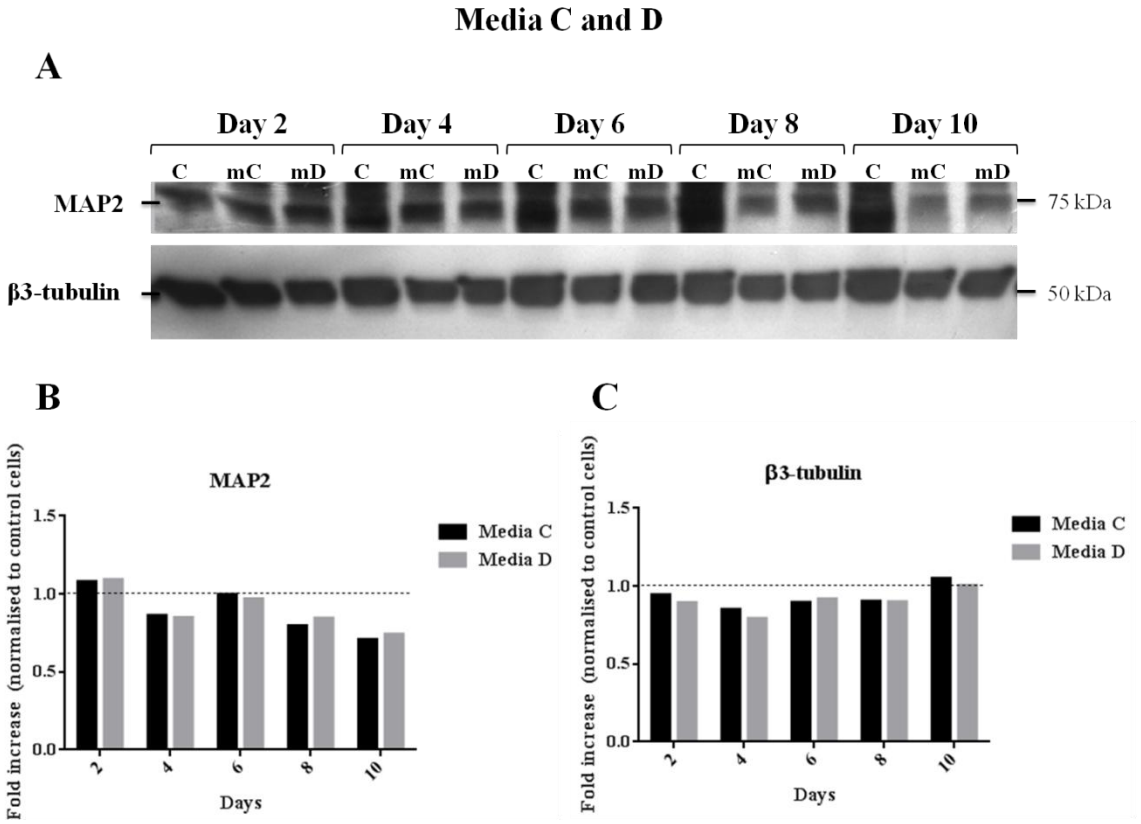

Figure 12 – Protein analysis of SH-SY5Y cells grown in media C and D. A. Western blot analysis of control SH-SY5Y cells and cells differentiated for 10 days using media C and D. **B.** Comparison of MAP2 between control cells and cells grown in media C and D. **C.** Comparison of β3-tubulin between control cells and cells grown in media C and D. Data was normalized to control levels for better comparison. All data was normalized to Ponceau S levels prior to analysis. C, control; mC, media C; mD, media D.

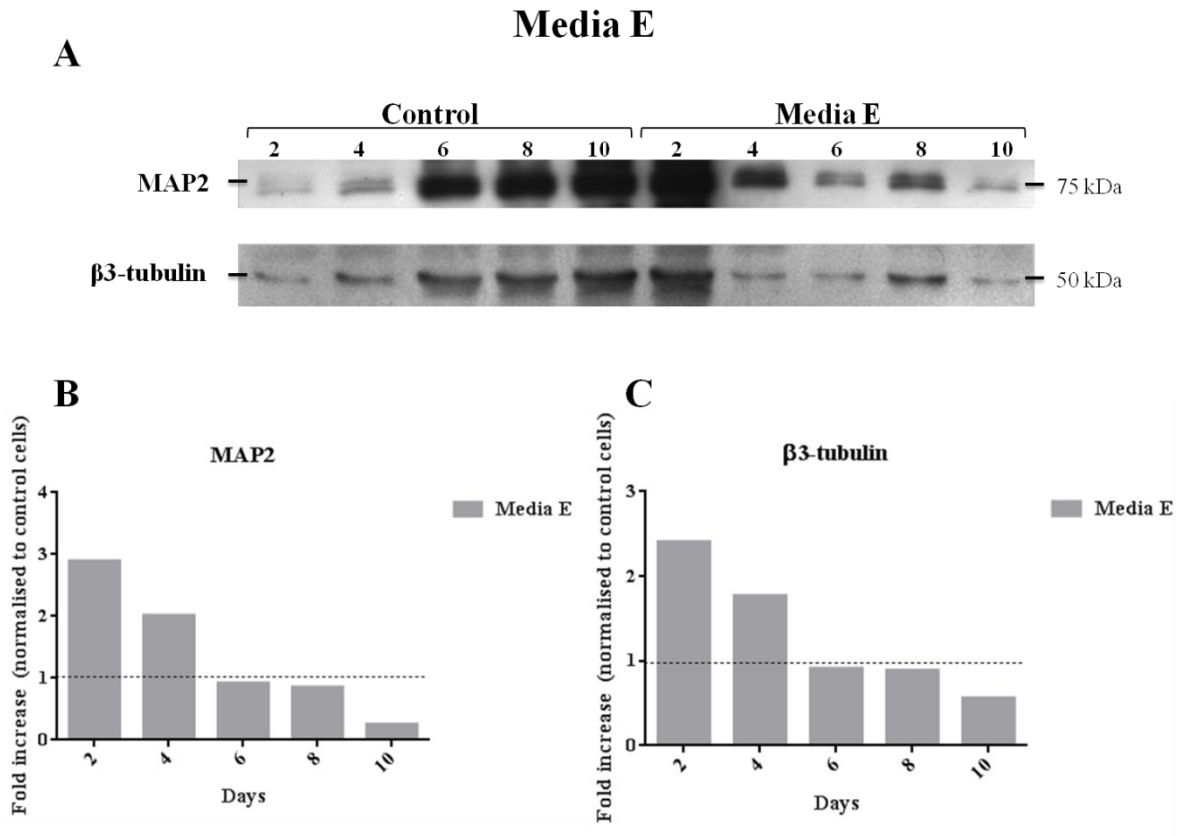

Figure 13 – Protein analysis of SH-SY5Y cells grown in media E. A. Western blot analysis of control SH-SY5Y cells and cells differentiated for 10 days using media E. **B.** Comparison of MAP2 between control and cells grown in media E. **C.** Comparison of β3-tubulin between control and cells grown in media E. Data was normalized to control levels for better comparison. All data was normalized to Ponceau S levels prior to analysis.

By analyzing Figure 12 it is possible to conclude the same as previous seen in the morphological analysis. Cells grown in media C and D did not exhibit many differences between them at the protein expression levels. By comparing both media with the controls, it is possible to observe that all three media exhibited roughly the same protein expression levels.

Cells grown in media E showed an increased expression of both MAP2 and β3-tubulin compared to the controls in the initial days (Figure 13). In the following days (6^{th} and 8^{th}), both MAP2 and β3-tubulin expression levels in control cells and cells grown in media E were similar, with control cells in the 10^{th} day having a higher expression of both markers. Since cells grown in media E began to die from the 4^{th} day onwards and control cells began to exhibit extended neurites when cultured for more than 4 days, this likely explains why the neuronal markers expression was similar between both control and cells grown in media E after the 4^{th} day.

Concluding, cells grown in media C and D did not exhibit many differences compared to the controls, while media E exhibited more neuronal markers expression in the initial days (2^{nd} and 4^{th}).

Thus, and by analyzing both the morphological changes and the protein markers expression, it was concluded that media E would be the most appropriate media for inducing SH-SY5Y differentiation. Additionally, since cells began to die from the 4^{th} day onward and the Aβ treatment requires 24 hours of culture, it was decided that cells would be cultured in media E for 2 days.

4.2. Aβ effect on neurabins expression

Aβ is a neurotoxic peptide which can lead to spine and synapse degeneration. Even when Aβ is applied extracellularly to SH-SY5Y cells, it is taken up by these cells, causing mitochondria damage [89] and neurite damage [107], events that ultimately lead to spine degeneration.

Since neurabin-1 and neurabin-2 are highly concentrated in the spine, especially in the PSD [29,73], and are important to spine morphogenesis and spine dynamics [27,38,52], their expression could be decreased in situations where this toxic peptide is present.

To test so, rat primary hippocampal cultures were cultured as described in section 3.2.4 and WB analysis was performed to assess both neurabin-1 and neurabin-2 expression (Figure 14). Additionally, the same analysis was performed in SH-SY5Y cells grown in media E to assess whether the SH-SY5Y culture behaved as the primary culture (Figure 15), thus allowing one to conclude whether this cell type would be suitable for neurabin-1 and neurabin-2 analysis.

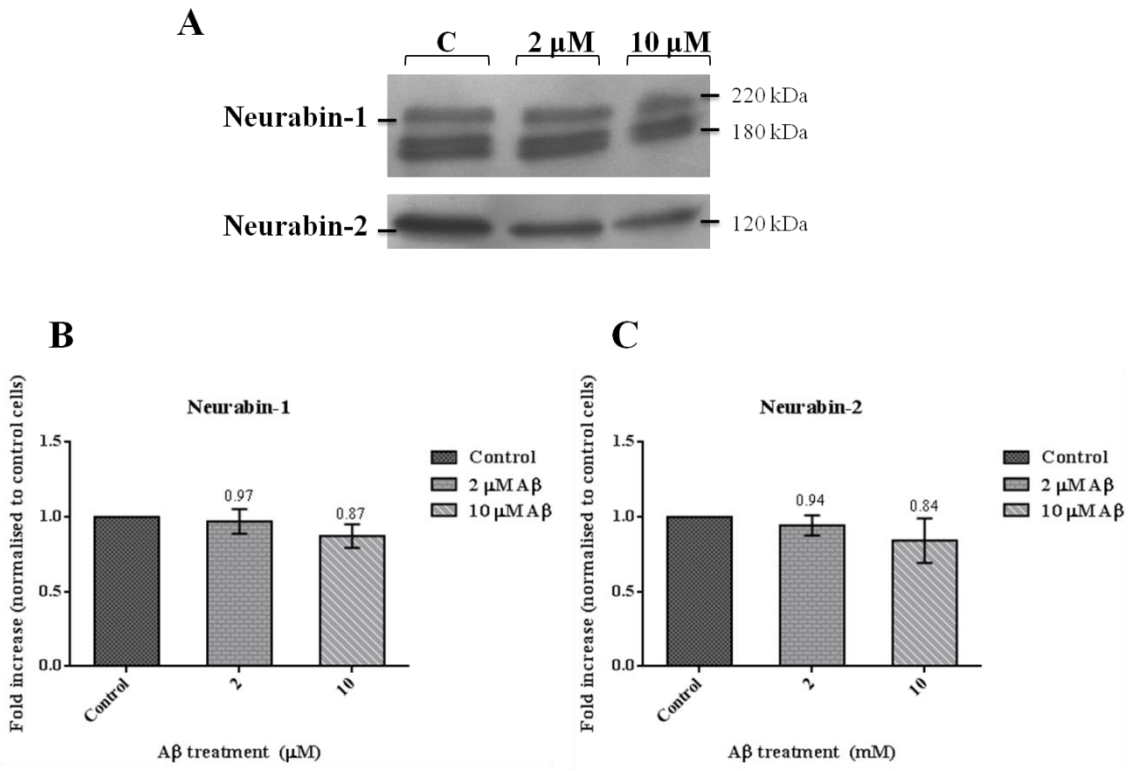

Figure 14 – Neurabin-1 and neurabin-2 expression in rat primary hippocampal cultures treated with Aβ1-42. A. Western blot of rat hippocampus lysates treated with different concentration of $A\beta_{1-42}$. **B.** Comparison of neurabin-1 expression in cells with different types of $A\beta_{1-42}$ treatment. **C.** Comparison of neurabin-2 expression in cells with different types of $A\beta_{1-42}$ treatment. C, 2 and 10 represents control cells and cells treated with 2 and 10 µM of $A\beta_{1-42,}$ respectively. All data was normalized to Ponceau S levels prior to analysis. Horizontal bars on B and C represent standard deviation, n = 3 (1-way ANOVA).

By analyzing Figure 14B it is possible to identify a tendency to decrease in neurabin-1 expression, perhaps due to the loss of synapses and dendritic spines typically caused by Aβ exposure, as seen in AD patients.

The results obtained with neurabin-2 (Figure 14C) point to a decrease in its expression in cells treated with $A\beta_{1-42}$ at high concentrations (10 μM). Several studies used this protein as a marker for spine density in transgenic mice with enhanced production of Aβ, and concluded that this protein is greatly reduced [108–110]. Thus, the tendency to decrease, seen here, is in agreement with the results obtained by other groups, which helps to speculate that the rat primary hippocampal cultures treated with 10 μM of $A\beta_{1-42}$ may have few number of spines compared to the controls. However, to properly conclude this, more samples need to be analyzed.

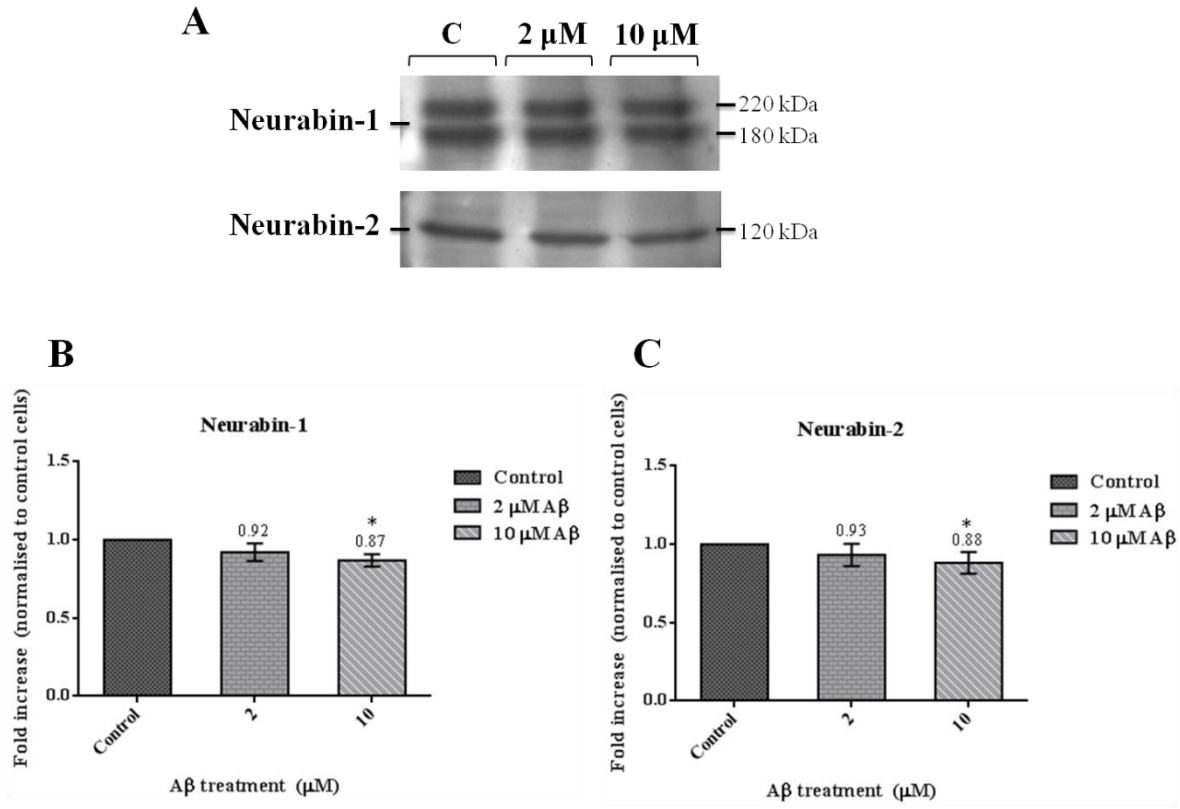

Figure 15 – Neurabin-1 and neurabin-2 expression in SH-SY5Y cells treated with Aβ1-42. A. WB analysis of SH-SY5Y lysates treated with different concentration of Aβ1-42. **B**. Comparison of neurabin-1 expression in cells with different types of Aβ1-42 treatment. **C.** Comparison of neurabin-2 expression in cells with different types of Aβ1-42 treatment. C, 2 and 10 represents control cells and cells treated with 2 and 10 μM of Aβ1-42, respectively. All data was normalized to Ponceau S levels prior to analysis. Horizontal bars on B and C represent standard deviation, n = 4, *p < 0.05 (1-way ANOVA).

The results obtained with the SH-SY5Y cells showed a slight decrease in the expression of both neurabins ($p < 0.05$), in agreement with the tendency to decrease seen with the primary cultures previously tested. This decrease could be due to the synaptic dysfunction caused by Aβ and consequently, dendritic spine degeneration [89].

The results here obtained with both primary cultures and SH-SY5Y cells suggest that in AD, these proteins' expression levels may be decreased, which could lead to a dysregulation of the actin dynamics of dendritic spines. This dysregulation can ultimately lead to dendritic spine and synaptic loss, leading to neuronal death and the clinically changes seen in AD [89,95].

4.3. Aβ effect on the neurabins/PP1 complex

Both neurabin-1 and neurabin-2 can interact with PP1 in order to regulate several aspects of neuronal morphology and synaptic plasticity [39,40,64,67]. Since cells treated with $A\beta_{1-42}$ are known to undergo both morphological and synaptic changes (dendritic spine degeneration, increase of LTD, decrease of LTP and neuronal death) [89], we tested whether $A\beta_{1-42}$ interferes with the interaction between neurabin-1/2 and PP1.

To do so, we performed a Co-IP with both PP1α and PP1γ and, through WB, tested the interactions between these PP1 and neurabin-1/2. The following images (Figure 16 and Figure 17) represent the results obtained.

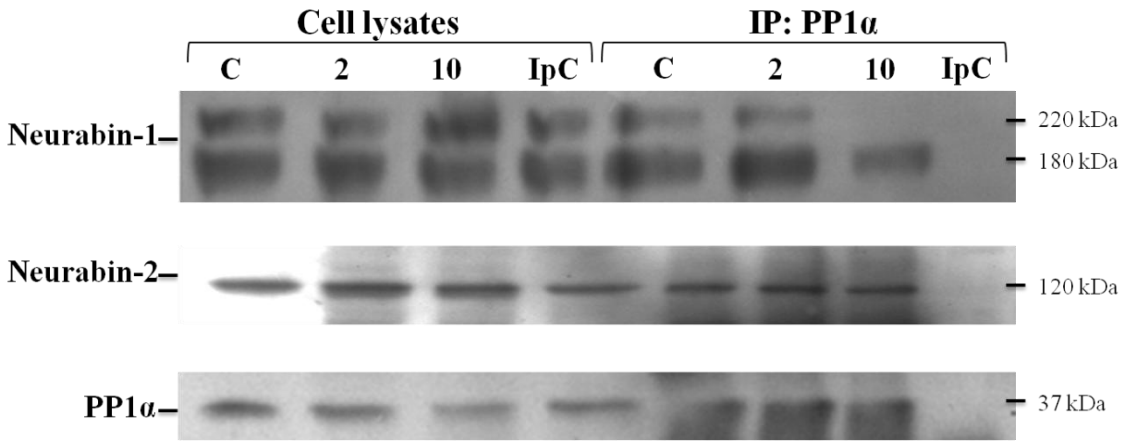

Figure 16 – Co-immunoprecipitation of PP1α binding proteins in SH-SY5Y. Western blot was performed using anti-PP1α to ensure that PP1α was immunoprecipitated, and anti-neurabin-1 and anti-neurabin-2 antibodies to test their interaction with PP1α. C, controls; 2 and 10, treatment with 2 and 10 μM $A\beta_{1-42}$, respectively; IpC, immunopreciptation controls.

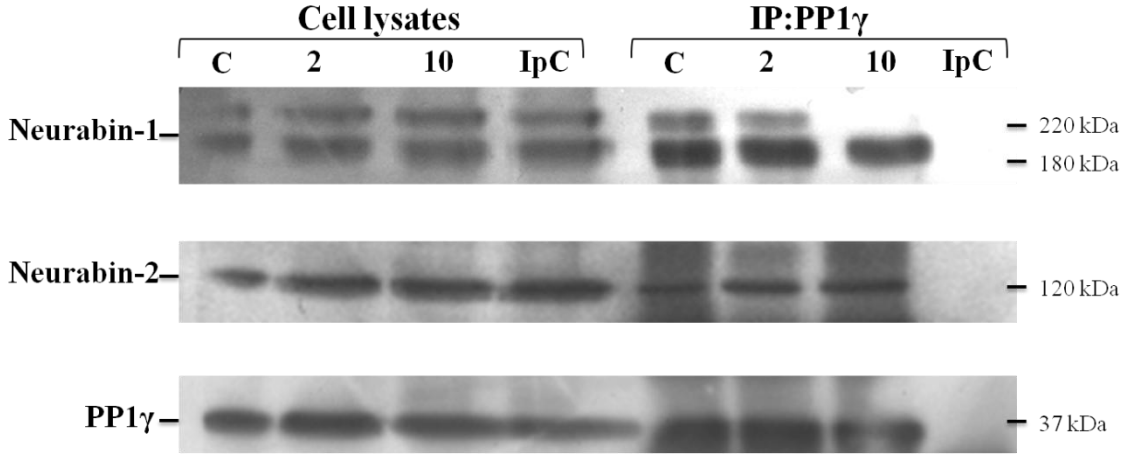

Figure 17 – Co-immunoprecipitation of PP1γ binding proteins in SH-SY5Y. Western blot was performed using anti-PP1γ to ensure that PP1γ was immunoprecipitated, and anti-neurabin-1 and anti-neurabin-2 antibodies to test their interaction with PP1γ. C, controls; 2 and 10, treatment with 2 and 10 μM $A\beta_{1-42}$, respectively; IpC, immunoprecipitation controls.

The results here obtained point to a change in the interaction between neurabin-1 and both PP1α and PP1γ, as one of the bands representing neurabin-1 (top one) failed to appear in cells treated with $A\beta_{1-42}$.

Several articles pointed to the existence of several bands when detecting neurabin-1 through WB, suggesting that the two lower bands (two almost united bands, can be distinguished in Figure 14A) could be proteolytic products of neurabin-1 [24,37,46,48]. If this assumption is correct, then perhaps $A\beta_{1-42}$ at high concentrations could interfere with full-length neurabin-1, inducing a conformational change that "hides" the PP1 binding motif, thus preventing its binding.

$A\beta_{1-42}$ could also induce physiological signals that increase full-length neurabin-1 interaction with another protein, thus displacing PP1 from its binding motif. In fact, it has been shown that cytosolic neurabin-1 (without its actin-binding domain) displays a decreased PP1 binding and recruits other proteins to the PDZ domain, such as p70S6K [27], so a similar mechanism could also be happening here when Aβ is present in the cells.

Additionally, $A\beta_{1-42}$ could also increase the activity of several kinases which, in turn, phosphorylate full-length neurabin-1, thus reducing its affinity for PP1. It is known that the activity of several protein kinases and protein phosphatases in the brains of AD patients is altered. ERK2 and Cdk5 in particular, are known to be increased [111], while PKA, the only reported kinase able to reduce neurabin-1 affinity for PP1 [27,46], is decreased [111]. Thus, it is unlikely that PKA could be the one causing the effects seen on the neurabin-1/PP1 complex. As for ERK2 and Cdk5, none of these kinases was reported as being able to phosphorylate neurabin-1 in a way that reduces its affinity for

PP1 [28,74]. Using the Group-based Prediction System 3.0 (GPS 3.0) [112], it was found that neurabin-1 has several predicted phosphorylation sites by several kinases which have their activity increased in AD patients. However, so far, these predicted phosphorylation sites were not tested *in vitro*/*in vivo*.

Furthermore, it is known that both PP1 expression [111,113] and activity [114] is decreased when Aβ is added to the cells. Thus, these disruptions could be due to the cumulative decrease of both PP1s and neurabin-1 expression in cells treated with Aβ, although we believe that this is unlikely since the decrease of both PP1s and neurabin-1 is not high enough to completely hinder the interaction between them.

However, as of today, none of the bands representing neurabin-1 was individually analyzed. Thus, it is impossible to conclude whether the above assumptions could be correct.

As for neurabin-2, its interaction with both PP1α and PP1γ does not seem to be affected by treatment with both 2 and 10 μM of $A\beta_{1-42}$, since no significant change was seen in neurabin-2's expression.

Why does the neurabin-1/PP1 complex seem to be affected while the neurabin-2/PP1 complex is not? Even though it has been suggested that these two proteins (neurabin-1 and neurabin-2) are regulators of each other in neurons, they can also interact with different proteins and can be phosphorylated by different kinases. Thus, this difference in the interacting partners could explain why Aβ affects each complex in a different manner.

4.4. Immunocytochemistry of SH-SY5Y cells treated with $A\beta_{1-42}$

In order to visualize *in vivo* whether the neurabin-1/PP1 complex was being disrupted by the addition of Aβ, we decided to perform an immunocytochemistry and determine the co-localization of neurabin-1 and both PP1α and PP1γ. These experimental procedures also permitted characterizing the cellular distribution of both neurabins.

The following images (Figure 18, Figure 19 and Figure 20) represent the results obtained.

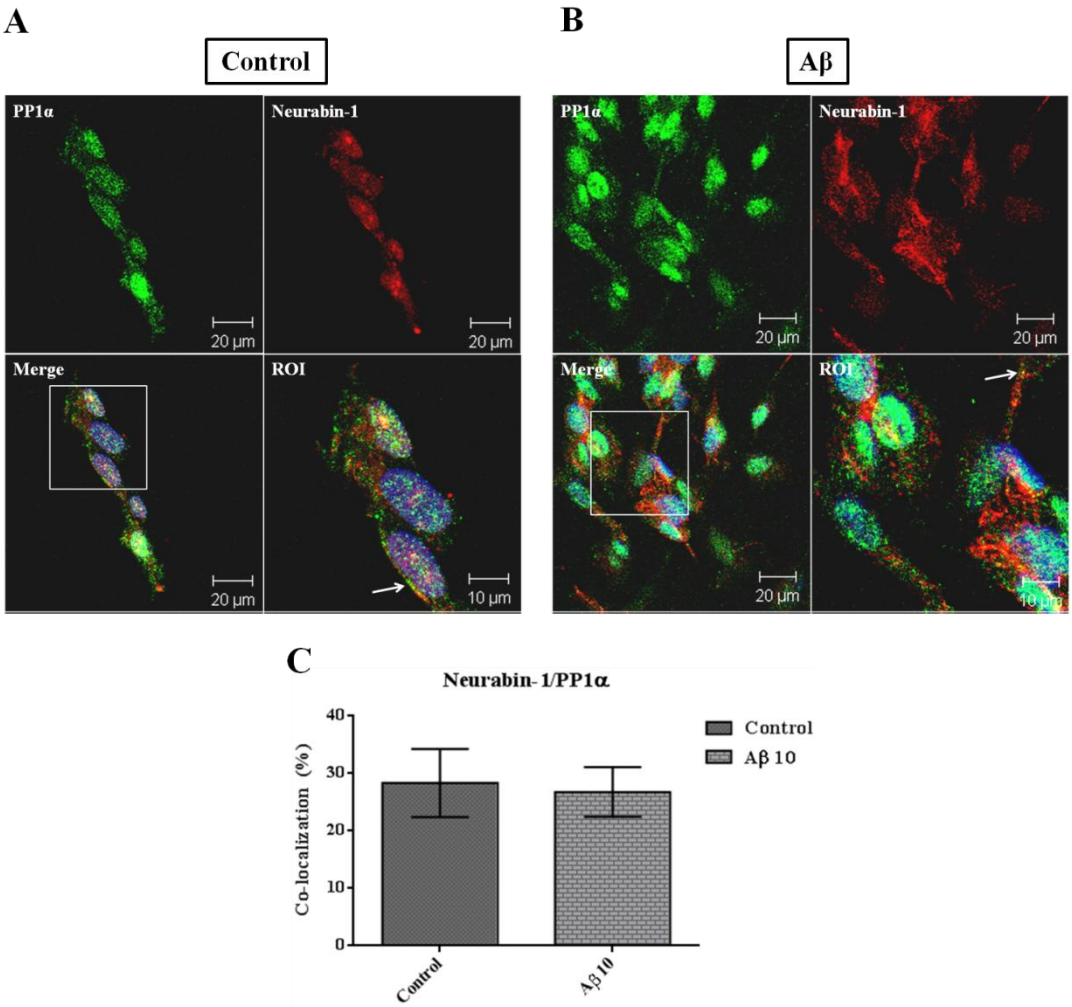

Figure 18 – PP1α and neurabin-1 localization in SH-SY5Y cells. PP1α appears as green, neurabin-1 as red. Blue represents the nucleus of the cells stained with DAPI. ROI represents the area within the white square on merge. White arrow points to an area where both proteins co-localize. **A.** Control cells. **B.** SH-SY5Y cells treated with 10 μM $A\beta_{1-42}$. **C.** Co-localization analysis. Results are represented as the mean percentage of all cells analyzed for each condition (controls, n = 79; cells treated with Aβ, n = 101).

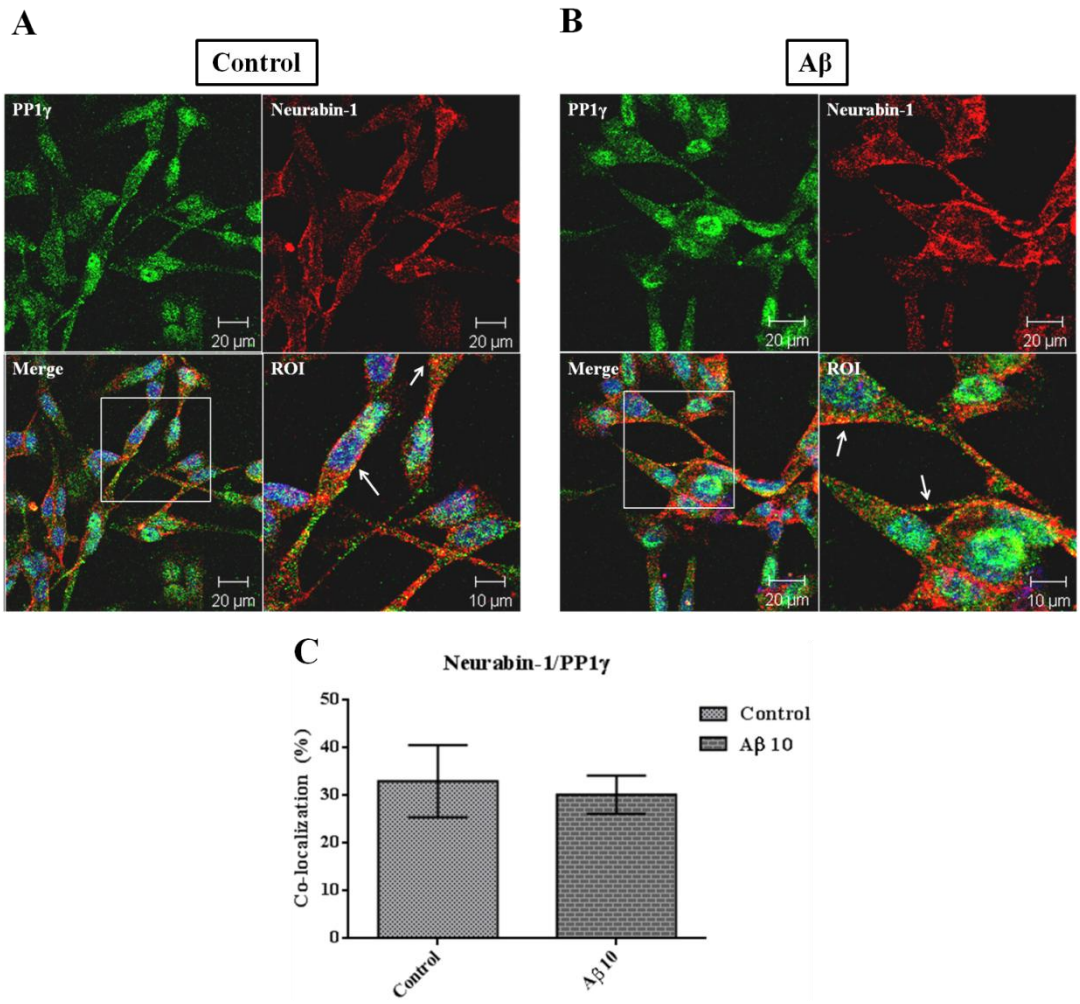

Figure 19 – PP1γ and neurabin-1 localization in SH-SY5Y cells. PP1γ appears as green, neurabin-1 as red. Blue represents the nucleus of the cells stained with DAPI. ROI represents the area within the white square on merge. White arrow points to an area where both proteins co-localize. **A.** Control cells. **B.** SH-SY5Y cells treated with 10 µM $A\beta_{1-42}$. **C.** Co-localization analysis. Results are represented as the mean percentage of all cells analyzed for each condition (controls, n = 91; cells treated with Aβ, n = 85).

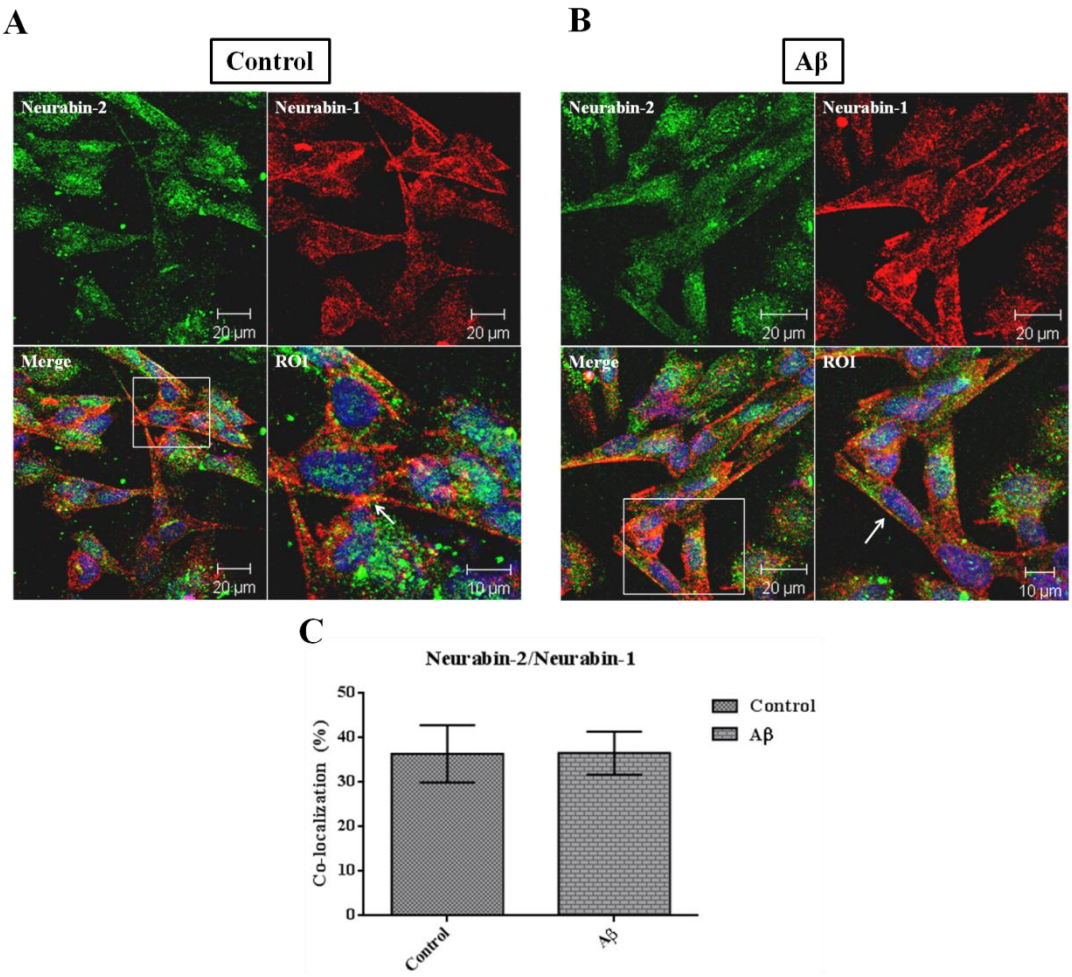

Figure 20 – Neurabin-2 and neurabin-1 localization in SH-SY5Y cells. Neurabin-2 appears as green, neurabin-1 as red. Blue represents the nucleus of the cells stained with DAPI. ROI represents the area within the white square on merge. White arrow points to an area where both proteins co-localize. **A.** Control cells. **B.** SH-SY5Y cells treated with 10 µM $A\beta_{1-42}$. **C.** Co-localization analysis. Results are represented as the mean percentage of all cells analyzed for each condition (controls, n = 62; cells treated with Aβ, n = 59).

By analyzing the above figures (Figure 18, Figure 19 and Figure 20) it is possible to observe that neurabin-1 (marked as red) is highly concentrated in the neurites, where the intensity of the signal was more intense. It also appears to be highly concentrated in the area surrounding the cytoplasm and within some regions in the cells, perhaps the cell membrane and the actin cytoskeleton, respectively, since neurabin-1 is known to interact with several proteins present in the cell membrane [36,50] and with F-actin [24,27]. Neurabin-2, as neurabin-1, can be found in the neurites, perhaps bound to F-actin. However, it seems to be more distributed within the cytoplasm than neurabin-1. The cellular distribution of both neurabin-1 and neurabin-2 does not seem to be affected by the treatment with $A\beta_{1-42}$.

In neurons, PP1α is mostly found within dendritic spines and also found in the cytoplasm and in the nucleus, while PP1γ is highly concentrated in dendritic spines and presynaptic terminals [18]. In the work here performed with SH-SY5Y cells, PP1α (marked as green on Figure 18) was found to be more expressed in the nucleus and in the cytoplasm, with little expression in the neurites. On the other hand, PP1γ (marked as green on Figure 19) was found to be more expressed in the neurites than PP1α, but could also be found in the nucleus and cytoplasm.

The co-localization analysis did not reveal any differences between control cells and cells treated with $A\beta_{1-42}$. The main aims of these experimental procedures were to assess neurabin-1 and PP1 co-localization in the presence of $A\beta_{1-42}$; and to observe whether neurabin-1 would be affected by $A\beta_{1-42}$ in terms of cellular localization. With the results here reported, we could not observe any differences between the co-localization of neurabin-1 and both PP1s and we did not see any major difference in the localization of neurabin-1. The results obtained with neurabin-2 also did not reveal any differences between control cells and cells treated with $A\beta_{1-42}$.

Fluorescence microscopy is a reliable technique to determine if two proteins can be found in the same cellular compartments and, when they co-localize, this supports a physical interaction *in vivo*. The resolution of a microscope is not sufficient to identify the physical interaction of two molecules through a comparison of their distributions in fluorescence images. Such studies require higher resolution techniques such as fluorescence resonance energy transfer or electron microscopy. Additionally, co-localization analysis can be influenced by background, i.e., low signal levels in the image derived from autofluorescence and nonspecific labeling [103]. This background can be eliminated in the acquisition process. Furthermore, the JACoP plugin permits the setting of a threshold to determine what we believe to be "true" signal, thus eliminating these non-specific signals when analyzing the images. Thus, arising from the fact that fluorescence microscopy is not the best approach to quantify the physical interaction between two proteins, and the co-localization analysis done afterwards can be prone to subjective errors, it is possible to explain why no differences were seen in the co-localization of neurabin-1 and both PP1s, i.e., differences between their interactions.

Nevertheless, the experimental procedure here performed was a preliminary study to assess the cellular distribution of neurabin-1 and neurabin-2 in SH-SY5Y cells, and further studies using higher resolution techniques are required in order to properly quantify the physical interaction between neurabin-1 and both PP1s, when Aβ is added to the cells.

5. Conclusion

This thesis aimed to evaluate whether Aβ could affect neurabin-1 and neurabin-2 expression, and disrupt or affect the neurabins/PP1 complex, which is important for the regulation of synaptic transmission, hippocampal plasticity and maintenance of dendritic spine morphology. These functions are known to be impaired in AD patients, therefore, studying all the molecular targets that could be affected by the overproduction of Aβ, particularly those known to be important in proper synaptic transmission, plasticity and dendritic spine morphology could help us to have a better understanding of the changes that occur in AD.

The experiments performed in this work with rat primary hippocampal cultures pointed to a slight decrease in both neurabin-1 and neurabin-2 expression when these cells were treated with $A\beta_{1-42}$ at a concentration of 10 μM. Additionally, the experiments performed with differentiated SH-SY5Y cells showed a significant decrease in both neurabins expression when treated with $A\beta_{1-42}$. These results suggest that neurabins expression in AD patients is decreased, perhaps due to the loss of synapses and dendrites (the locus of the majority of both neurabins localization) or due to the neuronal death that accompanies these latter changes. Whether neurabin-1 and neurabin-2 decreased expression is the result of the Aβ effects on the neurabins themselves or the result of the neuronal death triggered by Aβ could not be assessed at this point.

Our Co-IP results showed that the neurabin-1/PP1 complex seems to be affected when $A\beta_{1-42}$ is added to the media of the cells at a concentration of 10 μM, while the neurabin-2/PP1 complex did not seem to be affected by any of the $A\beta_{1-42}$ concentration. Based on these findings, we hypothesized three different models, which could link the disruptive effects of Aβ on the neurabin/PP1 complex to the changes seen in AD (Figure 21). However, none of these hypotheses could be confirmed at this point.

The immunocytochemistry here performed and the co-localization analysis did not demonstrate any differences between the co-localization of neurabin-1 and both PP1α and PP1γ when $A\beta_{1-42}$ was added to the cells. Moreover, $A\beta_{1-42}$ did not seem to affect the cellular distribution of neurabin-1 and neurabin-2, since no major differences were seen when compared to controls.

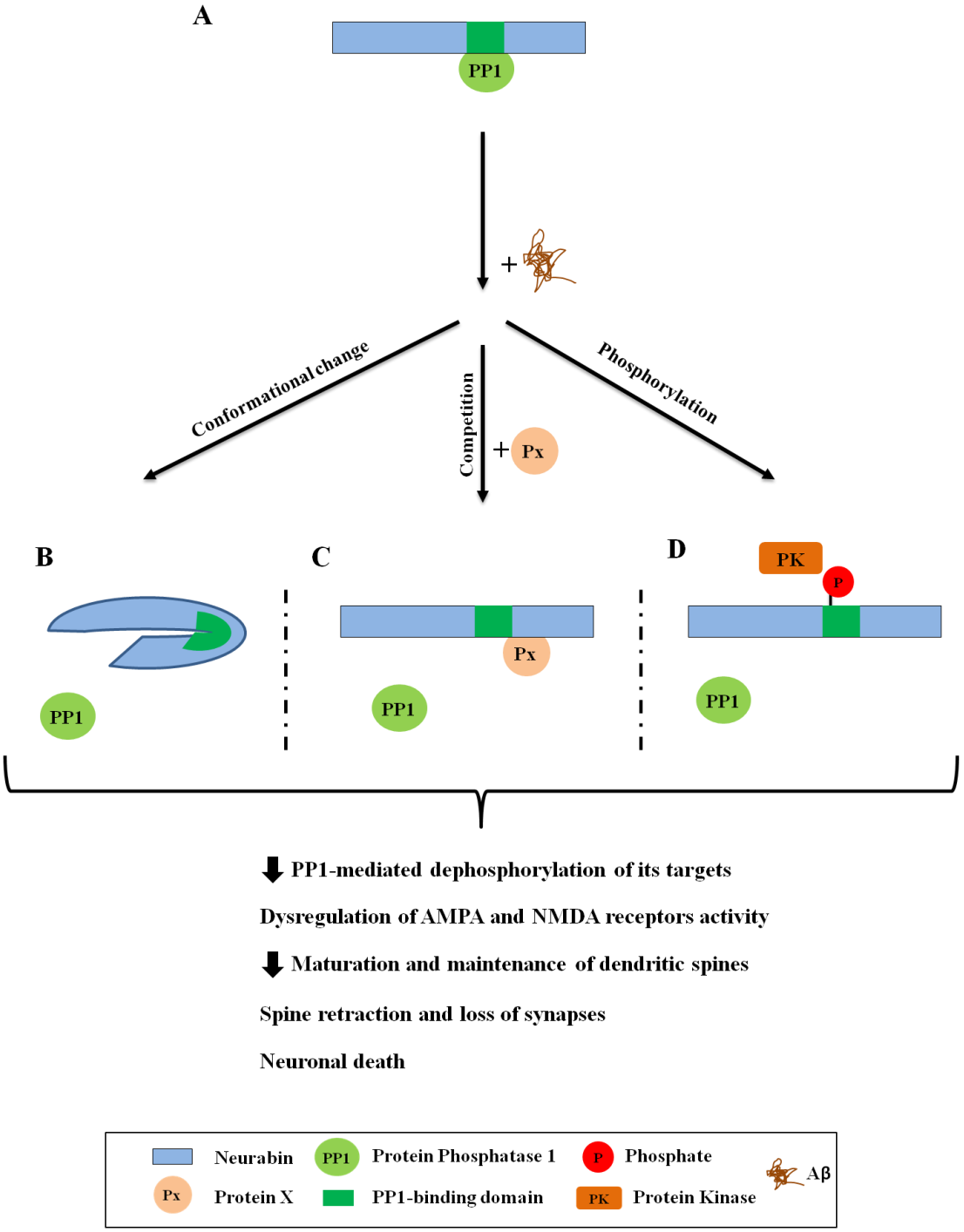

Figure 21 – Proposed models for the effect of Aβ on the neurabin/PP1 complex. The Aβ effects on the neurabin/PP1 complex would lead to changes in the spine dynamics which would eventually lead to synaptic loss and ultimately to neuronal death. **A.** Neurabin/PP1 complex under normal physiological conditions with PP1 bound to the PP1-binding domain of neurabin. **B.** Aβ could induce a conformational change in neurabin which would hide the PP1-binding domain. **C.** Aβ could increase neurabin's affinity for another protein (which binds to its PDZ domain, for example), displacing PP1 from its binding site. **D.** Aβ could increase the activity of a protein kinase, which would phosphorylate neurabin, displacing PP1 from its binding site.

Future Perspectives

In future works with neurabin-1, it would be of high importance to individually study what each band found in the WB analysis represents. This study would elucidate and help us understand the results obtained with our Co-IP. To do so, we could run a SDS-PAGE, cut the area where neurabin-1 can be found and submit it to mass-spectrometry analysis, which would identify the sequence of the protein present in each of the bands [115].

Additionally, it would be important to increase the number of experiments carried out with both rat primary hippocampal cultures and SH-SY5Y cells. This would increase the reliability of the results obtained with both neurabin-1 and neurabin-2 expression when cells were treated with Aβ. Moreover, it would be important to repeat the Co-IP in rat primary hippocampal cultures in order to reproduce the results obtained in SH-SY5Y cells.

It would also be interesting to increase the number of days that cells are treated with $A\beta_{1-42}$, as it would allows one to understand if the decrease seen with both neurabin-1 and neurabin-2 expression is proportional to the amount of time cells are exposed to Aβ.

Finally, it would be important to use microscopic techniques with higher resolution to compare the co-localization of neurabin-1 and both PP1s, such as electron microscopy, fluorescence resonance energy transfer [103] or proximity ligation assay [116].

6. References

1. Purves, D. *et al. Neuroscience*. (Sinauer Associates, Inc, 2011).

2. Bellot, A. *et al.* The structure and function of actin cytoskeleton in mature glutamatergic dendritic spines. *Brain Res.* **1573,** 1–16 (2014).

3. Adrian, M. *et al.* Barriers in the brain: resolving dendritic spine morphology and compartmentalization. *Front. Neuroanat.* **8,** 1–12 (2014).

4. Ethell, I. M. & Pasquale, E. B. Molecular mechanisms of dendritic spine development and remodeling. *Prog. Neurobiol.* **75,** 161–205 (2005).

5. Lamprecht, R. The actin cytoskeleton in memory formation. *Prog. Neurobiol.* **117C,** 1–19 (2014).

6. Hotulainen, P. & Hoogenraad, C. C. Actin in dendritic spines: Connecting dynamics to function. *J. Cell Biol.* **189,** 619–29 (2010).

7. Sala, C., Cambianica, I. & Rossi, F. Molecular mechanisms of dendritic spine development and maintenance. *Acta Neurobiol. Exp. (Wars).* **68,** 289–304 (2008).

8. Sheng, M. & Hoogenraad, C. C. The postsynaptic architecture of excitatory synapses: a more quantitative view. *Annu. Rev. Biochem.* **76,** 823–47 (2007).

9. Chia, P. H., Li, P. & Shen, K. Cell biology in neuroscience: cellular and molecular mechanisms underlying presynapse formation. *J. Cell Biol.* **203,** 11–22 (2013).

10. García-López, P., García-Marín, V. & Freire, M. Dendritic Spines and Development: Towards a Unifying Model of Spinogenesis - A Present Day Review of Cajal's Histological Slides and Drawings. *Neural Plast.* **2010,** 1–29 (2010).

11. Lai, K.-O. & Ip, N. Y. Structural plasticity of dendritic spines: the underlying mechanisms and its dysregulation in brain disorders. *Biochim. Biophys. Acta* **1832,** 2257–63 (2013).

12. Wu, L.-J. *et al.* Neurabin contributes to hippocampal long-term potentiation and contextual fear memory. *PLoS One* **3,** e1407 (2008).

13. Pontrello, C. G. & Ethell, I. M. Accelerators, Brakes, and Gears of Actin Dynamics in Dendritic Spines. *Open Neurosci. J.* **3,** 67–86 (2009).

14. Bollen, M., Peti, W., Ragusa, M. J. & Beullens, M. The extended PP1 toolkit : designed to create specificity. *Trends Biochem. Sci.* **35,** 450–8 (2011).

15. Heroes, E. *et al.* The PP1 binding code: a molecular-lego strategy that governs specificity. *FEBS J.* **280,** 584–95 (2013).

16. Ceulemans, H. & Bollen, M. Functional diversity of protein phosphatase-1, a cellular economizer and reset button. *Physiol. Rev.* **84,** 1–39 (2004).

17. Peti, W., Nairn, A. C. & Page, R. Structural Basis for Protein Phosphatase 1 Regulation and Specificity. *FEBS J.* **280,** 596–611 (2013).

18. Korrodi-Gregório, L., Esteves, S. L. C. & Fardilha, M. Protein phosphatase 1 catalytic isoforms: specificity toward interacting proteins. *Transl. Res.* **164,** 366–91 (2014).

19. Da Cruz e Silva, E. F. *et al.* Differential expression of protein phosphatase 1 isoforms in mammalian brain. *J. Neurosci.* **15,** 3375–89 (1995).

20. Braithwaite, S. P., Stock, J. B., Lombroso, P. J. & Nairn, A. C. Protein Phosphatases and Alzheimer's Disease. *Prog. Mol. Biol. Transl. Sci.* **106,** 343–79 (2012).

21. Hendrickx, A. *et al.* Docking Motif-Guided Mapping of the Interactome of Protein Phosphatase-1. *Chem. Biol.* **16,** 365–71 (2009).

22. Ragusa, M. J., Dancheck, B., Critton, D. a, Nairn, A. C. & Peti, W. Spinophilin directs Protein Phosphatase 1 specificity by blocking substrate binding sites. *Nat. Struct. Mol. Biol.* **17,** 459–64 (2010).

23. Hurley, T. D. *et al.* Structural basis for regulation of protein phosphatase 1 by inhibitor-2. *J. Biol. Chem.* **282,** 28874–83 (2007).

24. Nakanishi, H. *et al.* Neurabin: a novel neural tissue-specific actin filament-binding protein involved in neurite formation. *J. Cell Biol.* **139,** 951–61 (1997).

25. Nagase, T. *et al.* Prediction of the coding sequences of unidentified human genes. XV. The complete sequences of 100 new cDNA clones from brain which code for large proteins in vitro. *DNA Res.* **6,** 337–45 (1999).

26. UniProtKB - Q9ULJ8 (NEB1_HUMAN). at <http://www.uniprot.org/uniprot/Q9ULJ8>

27. Oliver, C. J. *et al.* Targeting Protein Phosphatase 1 (PP1) to the Actin Cytoskeleton : the Neurabin I / PP1 Complex Regulates Cell Morphology. *Mol. Cell. Biol.* **22,** 4690–701 (2002).

28. Futter, M. *et al.* Phosphorylation of spinophilin by ERK and cyclin-dependent PK 5 (Cdk5). *Proc. Natl. Acad. Sci. U. S. A.* **102,** 3489–94 (2005).

29. Muly, E. C. *et al.* Subcellular distribution of neurabin immunolabeling in primate prefrontal cortex: comparison with spinophilin. *Cereb. Cortex* **14,** 1398–407 (2004).

30. Nakabayashi, K. *et al.* Genomic imprinting of PPP1R9A encoding neurabin I in skeletal muscle and extra-embryonic tissues. *J. Med. Genet.* **41,** 601–8 (2004).

31. Allen, P. B., Ouimet, C. C. & Greengard, P. Spinophilin, a novel protein phosphatase 1 binding protein localized to dendritic spines. *Proc. Natl. Acad. Sci. U. S. A.* **94,** 9956–61 (1997).

32. Sarrouilhe, D. & Ladeveze, V. The tumour suppressor function of the scaffolding protein spinophilin. *Atlas Genet. Cytogenet. Oncol. Haematol.* **18,** 691–700 (2014).

33. Sarrouilhe, D., di Tommaso, a, Métayé, T. & Ladeveze, V. Spinophilin: from partners to functions. *Biochimie* **88,** 1099–113 (2006).

34. Barnes, A. P., Smith, F. D., VanDongen, H. M., VanDongen, A. M. J. & Milgram, S. L. The identification of a second actin-binding region in spinophilin/neurabin II. *Mol. Brain Res.* **124,** 105–13 (2004).

35. Satoh, A. *et al.* Neurabin-II/spinophilin. An actin filament-binding protein with one pdz domain localized at cadherin-based cell-cell adhesion sites. *J. Biol. Chem.* **273,** 3470–5 (1998).

36. Kelker, M. S. *et al.* Structural basis for spinophilin-neurabin receptor interaction. *Biochemistry* **46,** 2333–44 (2007).

37. Burnett, P. E. *et al.* Neurabin is a synaptic protein linking p70 S6 kinase and the neuronal cytoskeleton. *Proc. Natl. Acad. Sci. U. S. A.* **95,** 8351–6 (1998).

38. Terry-Lorenzo, R. T. *et al.* Neurabins recruit protein phosphatase-1 and inhibitor-2 to the actin cytoskeleton. *J. Biol. Chem.* **277,** 46535–43 (2002).

39. Terry-Lorenzo, R. T. *et al.* Neurabin / Protein Phosphatase-1 Complex Regulates Dendritic Spine Morphogenesis and Maturation. *Mol. Biol. Cell* **16,** 2349–62 (2005).

40. Hu, X. D., Huang, Q., Roadcap, D. W., Shenolikar, S. S. & Xia, H. Actin-associated neurabin-protein phosphatase-1 complex regulates hippocampal plasticity. *J. Neurochem.* **98,** 1841–51 (2006).

41. Chia, P. H., Patel, M. & Shen, K. NAB-1 instructs synapse assembly by linking adhesion molecules and F-actin to active zone proteins. *Nat. Neurosci.* **15,** 234–42 (2012).

42. Zito, K., Knott, G., Shepherd, G. M. G., Shenolikar, S. & Svoboda, K. Induction of spine growth and synapse formation by regulation of the spine actin cytoskeleton. *Neuron* **44,** 321–34 (2004).

43. Macmillan, L. B. *et al.* Brain actin-associated protein phosphatase 1 holoenzymes containing spinophilin, neurabin, and selected catalytic subunit isoforms. *J. Biol. Chem.* **274,** 35845–54 (1999).

44. Terry-Lorenzo, R. T. *et al.* The neuronal actin-binding proteins, neurabin I and neurabin II, recruit specific isoforms of protein phosphatase-1 catalytic subunits. *J. Biol. Chem.* **277,** 27716–24 (2002).

45. Stephens, D. J. & Banting, G. Direct Interaction of the trans-Golgi Network Membrane Protein, TGN38, with the F-actin Binding Protein, Neurabin. *J. Biol. Chem.* **274,** 30080–6 (1999).

46. Mcavoy, T. *et al.* Regulation of Neurabin I Interaction with Protein Phosphatase 1 by Phosphorylation. *Biochemistry* **38,** 12943–9 (1999).

47. Penzes, P. *et al.* The neuronal Rho-GEF Kalirin-7 interacts with PDZ domain-containing proteins and regulates dendritic morphogenesis. *Neuron* **29,** 229–42 (2001).

48. Orioli, D. *et al.* Rac3-induced Neuritogenesis Requires Binding to Neurabin I. *Mol. Biol. Cell* **17,** 1018–32 (2006).

49. Ryan, X. P. *et al.* The Rho-specific GEF Lfc interacts with neurabin and spinophilin to regulate dendritic spine morphology. *Neuron* **47,** 85–100 (2005).

50. Wang, X. *et al.* Spinophilin/neurabin reciprocally regulate signaling intensity by G protein-coupled receptors. *EMBO J.* **26,** 2768–76 (2007).

51. Stephens, D. J. & Banting, G. In vivo dynamics of the F-actin-binding protein neurabin-II. *Biochem. J.* **345,** 185–94 (2000).

52. Feng, J. *et al.* Spinophilin regulates the formation and function of dendritic spines. *Proc. Natl. Acad. Sci. U. S. A.* **97,** 9287–92 (2000).

53. Grossman, S. D., Hsieh-Wilson, L. C., Allen, P. B., Nairn, A. C. & Greengard, P. The actin-binding domain of spinophilin is necessary and sufficient for targeting to dendritic spines. *Neuromolecular Med.* **2,** 61–9 (2002).

54. Hsieh-Wilson, L. C. *et al.* Phosphorylation of spinophilin modulates its interaction with actin filaments. *J. Biol. Chem.* **278,** 1186–94 (2003).

55. Allen, P. *et al.* Control of protein phosphatase I in the dendrite. *Biochem. Soc. Trans.* **27,** 543–6 (1999).

56. Tsukada, M., Prokscha, A., Ungewickell, E. & Eichele, G. Doublecortin association with actin filaments is regulated by neurabin II. *J. Biol. Chem.* **280,** 11361–8 (2005).

57. Bielas, S. L. *et al.* Spinophilin Facilitates PP1-Mediated Dephosphorylation of PSer297 Doublecortin in Microtubule Bundling at the Axonal 'Wrist'. *Cell* **129,** 579–91 (2007).

58. Shmueli, A. *et al.* Site-specific dephosphorylation of doublecortin (DCX) by protein phosphatase 1 (PP1). *Mol. Cell. Neurosci.* **32,** 15–26 (2006).

59. Tsukada, M., Prokscha, A. & Eichele, G. Neurabin II mediates doublecortin-dephosphorylation on actin filaments. *Biochem. Biophys. Res. Commun.* **343,** 839–47 (2006).

60. Tsukada, M., Prokscha, A., Oldekamp, J. & Eichele, G. Identification of neurabin II as a novel doublecortin interacting protein. *Mech. Dev.* **120,** 1033–43 (2003).

61. Baucum, A. J., Strack, S. & Colbran, R. J. Age-Dependent Targeting of Protein Phosphatase 1 to Ca2+/Calmodulin-Dependent Protein Kinase II by Spinophilin in Mouse Striatum. *PLoS One* **7,** e31554 (2012).

62. Grossman, S. D. *et al.* Spinophilin is phosphorylated by Ca2+/calmodulin-dependent protein kinase II resulting in regulation of its binding to F-actin. *J. Neurochem.* **90,** 317–24 (2004).

63. Buchsbaum, R. J., Connolly, B. A. & Feig, L. A. Regulation of p70 S6 kinase by complex formation between the Rac guanine nucleotide exchange factor (Rac-GEF) Tiam1 and the scaffold spinophilin. *J. Biol. Chem.* **278,** 18833–41 (2003).

64. Richman, J. G. *et al.* Agonist-regulated Interaction between α2-Adrenergic Receptors and Spinophilin. *J. Biol. Chem.* **276,** 15003–8 (2001).

65. Sarrouilhe, D. & Métayé, T. Regulation of G-Protein-Coupled Receptor Signalling by the Scaffolding Proteins Spinophilin/Neurabin 2 and Neurabin 1. *Curr. Chem. Biol.* **5,** 130–41 (2011).

66. Wang, X. *et al.* Spinophilin regulates Ca2+ signalling by binding the N-terminal domain of RGS2 and the third intracellular loop of G-protein-coupled receptors. *Nat. Cell Biol.* **7,** 405–411 (2005).

67. Smith, F. D., Oxford, G. S. & Milgram, S. L. Association of the D2 dopamine receptor third cytoplasmic loop with spinophilin, a protein phosphatase-1-interacting protein. *J. Biol. Chem.* **274,** 19894–900 (1999).

68. Fujii, S., Yamazoe, G., Itoh, M., Kubo, Y. & Saitoh, O. Spinophilin inhibits the binding of RGS8 to M1-mAChR but enhances the regulatory function of RGS8. *Biochem. Biophys. Res. Commun.* **377,** 200–4 (2008).

69. Kurogi, M., Nagatomo, K., Kubo, Y. & Saitoh, O. Effects of spinophilin on the function of RGS8 regulating signals from M2 and M3-mAChRs. *Neuroreport* **20,** 1134–9 (2009).

70. Yan, Z. *et al.* Protein phosphatase 1 modulation of neostriatal AMPA channels: regulation by DARPP-32 and spinophilin. *Nat. Neurosci.* **2,** 13–17 (1999).

71. Fourla, D. D., Papakonstantinou, M. P., Vrana, S. M. & Georgoussi, Z. Selective interactions of spinophilin with the C-terminal domains of the δ- and μ-opioid receptors and G proteins differentially modulate opioid receptor signaling. *Cell. Signal.* **24,** 2315–28 (2012).

72. Strack, S. & Hell, J. in *Struct. Funct. Organ. Synap. SE - 16* (Hell, J. & Ehlers, M.) 459–500 (Springer US, 2008).

73. Muly, E. C., Smith, Y., Allen, P. & Greengard, P. Subcellular Distribution of Spinophilin Immunolabeling in Primate Prefrontal Cortex: Localization to and within Dendritic Spines. *J. Comp. Neurol.* **469,** 185–97 (2004).

74. Causeret, F. *et al.* Neurabin-I Is Phosphorylated by Cdk5 : Implications for Neuronal Morphogenesis and Cortical Migration. *Mol. Biol. Cell* **18,** 4327–42 (2007).

75. Prince, M., Albanese, E., Guerchet, M. & Prina, M. *Alzheimer's Disease International: World Alzheimer Report 2014*. (2014).

76. Alzheimer's Association. 2014 Alzheimer' s Disease Facts and Figures. *Alzheimer's Dement.* **10,** (2014).

77. Tarawneh, R. & Holtzman, D. M. The clinical problem of symptomatic Alzheimer disease and mild cognitive impairment. *Cold Spring Harb. Perspect. Med.* **2,** 1–16 (2012).

78. Associação Alzheimer Portugal. Factos e Dados sobre a Doença de Alzheimer. (2015). at <http://alzheimerportugal.org/pt/text-0-18-79-187-fact-sheet>

79. Stelzmann, R. A., Schnitzlein, H. N. & Murtagh, F. R. An English translation of Alzheimer's 1907 paper, 'uber eine eigenartige erkankung der hirnrinde'. *Clin. Anat.* **8,** 429–31 (1995).

80. Kumar, A. & Singh, A. A review on Alzheimer' s disease pathophysiology and its management: an update. *Pharmacol. Reports* **67,** 195–203 (2015).

81. Bamburg, J. R. & Bloom, O. Cytoskeletal Pathologies of Alzheimer Disease. *Cell Motil. Cytoskeleton* **66,** 635–49 (2009).

82. Castellani, R. J., Rolston, R. K. & Smith, M. A. Alzheimer Disease. *Dis. a Mon.* **56,** 484–546 (2010).

83. Zhang, Y., Thompson, R., Zhang, H. & Xu, H. APP processing in Alzheimer's disease. *Mol. Brain* **4,** 1–13 (2011).

84. Bilkei-Gorzo, A. Genetic mouse models of brain ageing and Alzheimer's disease. *Pharmacol. Ther.* **142,** 244–57 (2014).

85. Iqbal, K. *et al.* Animal models of the sporadic form of Alzheimer's disease: Focus on the disease and not just the lesions. *J. Alzheimer's Dis.* **37,** 469–74 (2013).

86. Mayeux, R. & Stern, Y. Epidemiology of Alzheimer Disease. *Cold Spring Harb. Perspect. Med.* **2,** 1–18 (2012).

87. Reitz, C. & Mayeux, R. Alzheimer disease: Epidemiology, diagnostic criteria, risk factors and biomarkers. *Biochem. Pharmacol.* **88,** 640–51 (2014).

88. Lloret, A., Fuchsberger, T., Giraldo, E. & Viña, J. Molecular mechanisms linking amyloid beta toxicity and Tau hyperphosphorylation in Alzheimer's Disease. *Free Radic. Biol. Med.* **83,** 186–91 (2015).

89. Cavallucci, V., D'Amelio, M. & Cecconi, F. Aβ toxicity in Alzheimer's disease. *Mol. Neurobiol.* **45,** 366–78 (2012).

90. De-Paula, V., Radanovic, M., Diniz, B. S. & Forlenza, O. V. in *Protein Aggreg. Fibrillogenes. Cereb. Syst. Amyloid Dis. SE - 14* (Harris, J. R.) **65,** 329–52 (Springer Netherlands, 2012).

91. O'Brien, R. J. & Wong, P. C. Amyloid Precursor Protein Processing and Alzheimer's Disease. *Annu Rev Neurosci* **34,** 185–204 (2011).

92. Jacobsen, K. T. & Iverfeldt, K. Amyloid precursor protein and its homologues: A family of proteolysis-dependent receptors. *Cell. Mol. Life Sci.* **66,** 2299–318 (2009).

93. Zhang, H., Ma, Q., Zhang, Y. & Xu, H. Proteolytic processing of Alzheimer's β-amyloid precursor protein. *J. Neurochem.* **120,** 9–21 (2012).

94. Cerasoli, E., Ryadnov, M. G. & Austen, B. M. The elusive nature and diagnostics of misfolded Aβ oligomers. *Front. Chem.* **3,** 1–6 (2015).

95. Tu, S., Okamoto, S.-I., Lipton, S. A. & Xu, H. Oligomeric Aβ-induced synaptic dysfunction in Alzheimer's disease. *Mol. Neurodegener.* **9,** 1–12 (2014).

96. Burry, R. W. *Immunocytochemistry, A Practical Guide for Biomedical Research*. (Springer-Verlag New York, 2010).

97. GE Healthcare Life Sciences. *Western Blotting: Principles and Methods*. (2014).

98. Kovalevich, J. & Langford, D. Considerations for the Use of SH-SY5Y Neuroblastoma Cells in Neurobiology. *Neuronal Cell Cult. Methods Protoc.* **1078,** 35–44 (2013).

99. Henriques, A. G. *et al.* Complexing Aβ Prevents the Cellular Anomalies Induced by the Peptide Alone. *J. Mol. Neurosci. mn* **53,** 661–8 (2014).

100. Thermo Fisher Scientific Inc. Pierce™ BCA Protein Assay Kit. (2015). at <https://www.lifetechnologies.com/order/catalog/product/23225>

101. Falsone, S. F., Gesslbauer, B. & Kungl, A. in *Genomics Protoc. SE - 20* (Starkey, M. & Elaswarapu, R.) **439,** 291–308 (Humana Press, 2008).

102. Thermo Fisher Scientific, I. Dynabeads® Protein G Immunoprecipitation Kit. (2015). at <https://www.lifetechnologies.com/order/catalog/product/10007D>

103. Dunn, K. W., Kamocka, M. M. & McDonald, J. H. A practical guide to evaluating colocalization in biological microscopy. *Am. J. Physiol. Cell Physiol.* **300,** C723–C742 (2011).

104. Manders, E. M. M., Verbeek, F. J. & Aten, J. a. Measurement of Colocalization of Objects in Dual-Color Confocal Images. *J. Microsc.* **169,** 375–82 (1993).

105. Cheung, Y. T. *et al.* Effects of all-trans-retinoic acid on human SH-SY5Y neuroblastoma as in vitro model in neurotoxicity research. *Neurotoxicology* **30,** 127–35 (2009).

106. Brunner, D. *et al.* Serum-free cell culture: the serum-free media interactive online database. *ALTEX* **27,** 53–62 (2010).

107. Mokhtar, S. H., Bakhuraysah, M. M., Cram, D. S. & Petratos, S. The Beta-Amyloid Protein of Alzheimer's Disease: Communication Breakdown by Modifying the Neuronal Cytoskeleton. *Int. J. Alzheimers. Dis.* **2013,** 1–15 (2013).

108. Palavicini, J. P. *et al.* RanBP9 aggravates synaptic damage in the mouse brain and is inversely correlated to spinophilin levels in Alzheimer's brain synaptosomes. *Cell Death Dis.* **4,** e667 (2013).

109. Wang, H., Lewsadder, M., Dorn, E., Xu, S. & Lakshmana, M. K. RanBP9 overexpression reduces dendritic arbor and spine density. *Neuroscience* **265,** 253–62 (2014).

110. Wang, R. *et al.* RanBP9 overexpression accelerates loss of dendritic spines in a mouse model of Alzheimer's disease. *Neurobiol. Dis.* **69,** 169–79 (2014).

111. Chung, S. H. Aberrant phosphorylation in the pathogenesis of Alzheimer's disease. *BMB Rep.* **42,** 467–74 (2009).

112. Liu, Z. *et al.* GPS 3.0: web servers for the prediction of protein post-translational modification sites. **Submitted,** (2015).

113. Amador, F. C., Henriques, A. G., Da Cruz E Silva, O. a B. & Da Cruz E Silva, E. F. Monitoring protein phosphatase 1 isoform levels as a marker for cellular stress. *Neurotoxicol. Teratol.* **26,** 387–95 (2004).

114. Vintém, A. P. B., Henriques, A. G., da Cruz E Silva, O. a B. & da Cruz E Silva, E. F. PP1 inhibition by Abeta peptide as a potential pathological mechanism in Alzheimer's disease. *Neurotoxicol. Teratol.* **31,** 85–8 (2009).

115. Albright, J. C., Dassenko, D. J., Mohamed, E. a. & Beussman, D. J. Identifying gel-separated proteins using in-gel digestion, mass spectrometry, and database searching: Consider the chemistry. *Biochem. Mol. Biol. Educ.* **37,** 49–55 (2009).

116. Gullberg, M. & Andersson, A. Visualization and quantification of protein-protein interactions in cells and tissues. *Nat. Methods* **7,** 2 (2010).

7. Appendix

Cell Culture Solutions

- **PBS (1x)**

For a final volume of 500 mL, dissolve one pack of BupH Modified Dulbecco's Phosphate Buffered Saline Pack (Pierce) in deionised H_2O. Final composition:

  - 8 mM Sodium Phosphate
  - 2 mM Potassium Phosphate
  - 140 mM Sodium Chloride
  - 10 mM Potassium Chloride

Sterilize by filtering through a 0.2 μm filter and store at 4°C.

- **10% FBS MEM:F12 (1:1)**
  - 4.805 g MEM
  - 5.315 g F12
  - 1.5 g NaHCO3
  - 0.055 g Sodium Pyruvate
  - 10 mL Streptomycin/Penicillin/Amphotericin solution
  - 100 mL 10% FBS
  - 2.5 mL L-glutamine (200 mM stock solution)

Dissolve in deionised H_2O. Adjust the pH to 7.2-7.3. Adjust the volume to 1000 mL with deionised H_2O.

For other combinations of FBS, replace 100 mL FBS with 30 mL (3% FBS MEM:F12), 10 mL (1% FBS MEM:F12) or remove FBS (serum-free MEM:F12).

- **10 mg/mL Poly-D-lysine stock (100x)**

To a final volume of 10 mL, dissolve in deionesed H_2O 100 mg of poly-D-lysine (Sigma-Aldrich).

- **Borate buffer**

To a final volume of 1 L, dissolve in deionised H_2O 9.28 g of boric acid (Sigma-Aldrich). Adjust pH to 8.2, sterilize by filtering through a 0.2 μM filter, and store at 4°C.

- **Poly-D-lysine solution**

To a final volume of 100 mL, dilute 1 mL of the 10 mg/mL poly-D-lysine stock solution in borate buffer.

- **Hank's Balanced Salt Solution (HBSS)**

This salt solution is prepared with deionised H_2O. Final composition:

- 137 mM NaCl
- 5.36 mM KCl
- 0.44 mM KH_2PO_4
- 0.34 mM $Na_2HPO_42H_2O$
- 4.16 mM $NaHCO_3$
- 5 mM Glucose
- 1 mM Sodium Pyruvate
- 10 mM HEPES

Adjust pH to 7.4. Sterilize by filtering through a 0.2 μm filter and store at 4°C.

- **Complete Neurobasal medium**

This serum-free medium (Neurobasal; Gibco) is supplemented with:

- 2% B27 supplement
- 0.5 mM L-glutamine
- 25 μM L-glutamate
- 60 μg/mL Gentamicine
- 0.001% Phenol Red

Adjust pH to 7.4. Sterilize by filtering through a 0.2 μm filter and store at 4°C.

Western Blot Solutions

- **LGB (lower gel buffer) (4x)**

To 900 mL of deionised H_2O add:

- 181.65 g of Tris
- 4 g of SDS

Mix until the solutes have dissolved. Adjust pH to 8.9 and adjust the volume to 1 L with deionised H_2O.

- **UGB (Upper gel buffer) (4x)**

To 900 mL of deionised H_2O add:

  - 75.69 g of Tris

Mix until the solute has dissolved. Adjust the pH to 6.8 and adjust the volume to 1 L with deionised H_2O.

- **10% APS (ammonium persulfate)**

In 10 mL of deionised H_2O dissolve 1 g of APS. Note: prepare fresh before use.

- **10% SDS (sodium dodecilsulfate)**

In 10 mL of deionised H_2O dissolve 1 g of SDS.

- **Loading Gel Buffer (4x)**
  - 2.5 mL 1M Tris solution (pH 6.8) 2.5 mL (250 mM)
  - 0.8 g SDS (8%)
  - 4 mL Glicerol (40%)
  - 2 mL β-mercaptoethanol (2%)
  - 1 mg Bromofenol blue (0.01%)

Adjust the volume to 10 mL with deionised H_2O. Store in darkness at room temperature.

- **1 M Tris (pH 6.8) solution**

To 150 mL of deionised H_2O add:

  - 30.3 g Tris base

Adjust the pH to 6.8 and adjust the final volume to 250 mL with deionised H_2O.

- **10x Running Buffer**
  - 30.3 g Tris (250 mM)
  - 144.2 g Glycine (2.5 M)
  - 10 g SDS (1%)

  Dissolve in deionised H_2O, adjust the pH to 8.3 and adjust the volume to 1 L.

- **Stacking and resolving gel**

Type of Gel	Stacking	Resolving	
Polyacrylamide percentage	3.5 %	5 %	20 %
H_2O	13.2 mL	17.4 mL	2.2 mL
Acrylamide stock mixture	2.4 mL	5 mL	20 mL
UGB (5x)	4 mL	n/a	n/a
LGB (4x)	n/a	7.5 mL	7.5 mL
10% SDS	200 µL	n/a	n/a
10% APS	200 µL	150 µL	150 µL
TEMED	20 µL	15 µL	15 µL

- **Transfer Buffer (1x)**
  - 3.03 g Tris (25 mM)
  - 14.41 g Glycine (192 mM)

Mix until solutes dissolution. Adjust the pH to 8.3 with HCl and adjust the volume to 800 mL with deionised H_2O. Just prior to use add 200 mL of methanol (20%).

- **10x TBS (Tris buffered saline)**
  - 12.11 g Tris (10 mM)
  - 87.66 g NaCl (150 mM)

Adjust the pH to 8.0 with HCl and adjust the volume to 1 L with deionised H_2O.

- **10x TBST (TBS+Tween)**
  - 12.11 g Tris (10 mM)
  - 87.66 g NaCl (150 mM)
  - 10 mL Tween-20 (0.01%)

Adjust the pH to 8.0 with HCl and adjust the volume to 1 L with deionised H_2O.

- **Membranes Stripping Solution (500 mL)**
  - 3.76 g Tris-HCl (62.5 mM)
  - 10 g SDS (2%)
  - 3.5 mL β-mercaptoethanol (100 mM)

Dissolve Tris and SDS in deionised H_2O and adjust with HCl to pH 6.7. Add the β-mercaptoethanol and adjust volume to 500 mL.

- **Blocking solution**

To 20 mL of TBS 1x add 1 g of Bovine Serum Albumine (BSA).

Immunofluorescence Solutions

- **Blocking solution**

To 10 mL of PBS 1x add 0.3 g of Bovine Serum Albumine (BSA).

- **4% Paraformaldehyde**

For a final volume of 100 mL, add 4 g of paraformaldehyde to 25 mL deionised H_2O. Dissolve by heating the mixture at 58°C while stirring. Add 1-2 drops of 1 M NaOH to clarify the solution and filter through a 0.2 μM filter. Add 50 mL of PBS 2x and adjust the volume to 100 mL with deionised H_2O.